Update on a class of gradient theories

E.C. Aifantis [a,b,*]

[a] *Center for the Mechanics of Material Instabilities, and Manufacturing Processes (MMIMP), Michigan Technological University, Houghton, MI 49931, USA*

[b] *Laboratory of Mechanics and Materials (LMM), Polytechnic School, Aristotle University of Thessaloniki, P.O. Box 468, Thessaloniki 54124, Greece*

Abstract

This article, written in honor of Professor Nemat-Nasser, provides an update of the standard theories of dislocation dynamics, plasticity and elasticity properly modified to include scale effects through the introduction of higher order spatial gradients of constitutive variables in the governing equations of material description. Only a special class of gradient models, namely those developed by the author and his co-workers, are considered. After a brief review of the basic mathematical structure of the theory and certain gradient elasticity solutions for dislocation fields, the physical origin and form of the gradient terms (for all classes of elastic, plastic, and dislocation dynamics behavior), along with the nature of the associated phenomenological coefficients are discussed. Applications to the interpretation of deformation patterning and size effects are given. Two new features are noted: the role of wavelet analysis and stochasticity in interpreting deformation heterogeneity measurements and serrations of the stress–strain graph.
© 2002 Elsevier Science Ltd. All rights reserved.

1. Introduction

It is with sincere appreciation and considerable degree of admiration to the multifaceted and continuously evolving work of Professor Sia Nemat-Nasser that this update on gradient theory is dedicated to him for the influence he had upon the mechanics community and various areas of materials research that I have been working on. Gradient theory, of the form and scope dealt with

here, was introduced by the author and his co-workers in the beginning of 1980s to address problems on dislocation patterning, width/spacings of shear bands, and mesh-size independence of finite element calculations in the material softening regime. Prior to that there has been a large number of generalized continuum mechanics theories of gradient type based on mathematical extensions of the Cosserat continuum (multipolar, micropolar, micromorphic, nonlocal media) available in the literature, but they involved a long list of unspecified phenomenological constants and were mainly concerned with wave propagation studies. Thus, the central problem of material instabilities, the emergence and development of deformation patterns and associated plastic

---

[*] Address: Laboratory of Mechanics and Materials (LMM), Polytechnic School, Aristotle University of Thessaloniki, P.O. Box 468, Thessaloniki 54124, Greece. Fax: +30-310-995921.

E-mail address: mom@mom.gen.auth.gr (E.C. Aifantis).

heterogeneities were not addressed. In fact, due to the complexity of their mathematical structure, only the linearized version of these theories were used and material softening was excluded. As a result, the aforementioned material instability and inhomogeneity questions could not even be considered within the existing framework of the previously available gradient type theories. The gradient approach discussed here is based on the introduction of length scale effects in elasticity, plasticity and dislocation dynamics by incorporating higher order gradients (often the Laplacian) of strain and/or dislocation densities into the constitutive or evolution equations (for a recent review see Aifantis, 1999a,b, 2001) governing the material description. The resulting models of gradient dislocation dynamics or multi-element defect kinetics, gradient plasticity, and gradient elasticity have been proven very useful in describing dislocation patterning phenomena and the self-organization of structural defects, the width and spacing of shear bands, various types of size effects, as well as the details of the deformation field near dislocation/disclination lines and crack tips. These features could not be captured by classical theory. A brief critical review of gradient theory in view of recent developments in related fields is given below.

1.1. Gradient dislocation dynamics/multi-element defect kinetics

Bammann and Aifantis (1982) developed an initial model for plastic deformation including evolution equations for the dislocation densities of the reaction-diffusion type. This work was used later as a basis for the development of the W–N model (Walgraef and Aifantis, 1985) for mobile and immobile dislocations. The W–A model provided an estimate for the wavelength of persistent slip bands (PSBs) during cyclic deformation and described qualitatively the competition between veins and PSBs in fatigued metals. The diffusion-like coefficients for defect kinetics were initially calibrated from wavelength measurements of associated dislocation patterns for which standard dislocation dynamics models could not provide any information. This initial dislocation kinetics

model could be viewed as the original motivation for current work on dislocation patterning by using three-dimensional discrete dislocation dynamics (DDD), as pioneered originally by Kubin and co-workers (e.g. Kubin and Devincre, 1999, and references cited therein) and further elaborated upon later by Zbib et al. (1998c). In fact, DDD simulations may be used to calibrate numerically the form of the diffusion and reaction constants entering into the W–A model. Such expressions have been deduced recently on the basis of mechanism-based discrete microscopic models of defect interaction, production, and annihilation (e.g. Aifantis, 1999a,b; Zaiser and Aifantis, 1999). Subsequently to the initial success of the W–A model, Romanov and Aifantis (1993) have further elaborated upon the reaction-diffusion type of approach for dislocation species to incorporate other types of defects such as disclinations and immobile dislocation/disclination dipoles, thus producing a generalized scheme of defect kinetics for monotonic deformation. The resulting multi-element defect kinetics model was used to interpret the occurrence of slip and rotational bands during strain hardening of bulk crystals, the clustering of misfit dislocations in thin films, as well as periodic crack profiles in subcritical fracture. Of particular interest are the stability results on misfit dislocation clustering reported by the author and co-workers (Liosatos et al., 1998; Cholevas et al., 1998), as well as the more elaborate "reaction kinetics" results obtained along the same lines in a series of articles by Romanov in collaboration with the Santa Barbara group (Romanov et al., 1999; Romanov and Speck, 2000).

1.2. Gradient plasticity

Simultaneously with the gradient dynamics models, a strain gradient plasticity theory first suggested by the author (Aifantis, 1982, 1983, 1984b,c) and later elaborated upon by him (Aifantis, 1987, 1992, 1995, 1996) was used and further examined by Zbib and Aifantis (1988a,b) to determine the thickness of shear bands, as well as the spacing and velocity of Portevin-Le Chatelier bands. The simplest form of the strain gradient plasticity theory involves only one extra coefficient

incorporating the effect of the Laplacian of the equivalent shear strain into the constitutive expression for the flow stress. The extra gradient coefficient may be calibrated through shear band thickness measurements and size effect data interpretations for which classical plasticity could not provide any information. The form and magnitude of this extra gradient coefficient depends on the dominant mechanism of plastic flow at the scale under consideration. For plastically deformed polycrystals, self-consistent arguments can be used to derive an expression involving the average grain size, the elastic constants and the plastic hardening modulus (Aifantis, 1995). DDD simulations can also be used, in principle, to derive expressions for the gradient coefficient depending on the relevant microscopic configuration, and this task is currently under exploration. The aforementioned initial strain gradient plasticity theory has motivated extensive work on gradient-dependent strain softening solids since it eliminated the mesh-size dependence of finite element calculations (e.g. Belytschko and Kulkarni, 1991; Sluys and de Borst, 1994; Tomita, 1994), and allowed the development of computer codes to capture the occurrence of complex deformation patterns in the solution of related boundary value problems. Other types of strain gradient plasticity models based on the concept of geometrically necessary dislocations (GND), such as those advanced recently by Fleck et al. (1994) and Gao et al. (1999), are also being currently used by many investigators to interpret strengthening and size-dependent hardness measurements at the micron and nano scales.

1.3. Gradient elasticity

Due to the success of the aforementioned scale-dependent models for plasticity and defect kinetics, the theory of nonlinear elasticity was revisited by Triantafyllidis and Aifantis (1986) by allowing the second deformation gradient to enter into the strain energy function. The linearized version of the resulting stress–strain relation amounts into adding the Laplacian of the classical stress expression into the standard form of Hooke's law. The model was applied to eliminate the strain

singularity at dislocation lines and crack tips, thus providing the structure or morphology of dislocation cores and crack faces. In particular, the strain singularity from crack tips can be eliminated as shown, for example, by Altan and Aifantis (1992, 1997); Ru and Aifantis (1993) and Unger and Aifantis (1995, 2000). Smooth crack closure and Barenblatt-Dugdale type cohesion zones are naturally obtained within this theory, but also oscillatory crack profiles can be predicted (Unger and Aifantis, 2000), in agreement with some experimental observations. The strain singularity can also be eliminated from dislocation and disclination lines and estimates for the dislocation core sizes can be obtained as shown in a series of articles by Gutkin and Aifantis (1996, 1999a). A modified gradient elasticity model incorporating also stress gradients into the stress–strain law was utilized by Gutkin and Aifantis (1999b, 2000) more recently to eliminate both stress and strain singularities from dislocation lines and derive a new type of "image force" for a dislocation near an interface.

1.4. Gradients and size effects

Gradient-dependent constitutive equations can be used to consider the important issue of size effect, i.e. the dependence of strength and other mechanical properties on the size of the specimen. This may be physically understood on the basis that higher-order gradients in the constitutive variables is a measure of the heterogeneous character of deformation field, the overall effect of which may depend on the specimen size. In fact, solution of boundary value problems based on higher-order governing equations for the strain field bring in the size of the specimen in a non-trivial manner and, thus, related size effects may be captured accordingly. The ability of gradient elasticity and gradient plasticity to interpret such effects in torsion and bending of standard-sized specimens with uncommon microstructure or small-sized specimens with common microstructure, is discussed by the author (Aifantis, 1999b) within a simplified framework of a strength of materials approach. Additional results on modelling size effects in three-dimensional composites

and in micro/nano indentation are given in a recent review article of the author written for a handbook of materials behavior models (Aifantis, 2001). Due to the lack of macroscopic gradients during tension of uniform bars, size effects in this case cannot be interpreted by gradient theory without modifying it to account for localized strain heterogeneities. Such a modification may be accomplished by allowing the average value of a radially (for cylindrical smooth tensile specimens) or transversely (for flat smooth tensile specimens) evolving internal variable with diffusive transport in the respective direction to enter into the stress–strain relationship. Alternatively, size effects in tension may be interpreted by casting the gradient-dependent constitutive equation into a scale-dependent constitutive equation through the use of wavelet analysis. The gradient term is then replaced by a scale term which depends on the ratio of the internal over the gage length and reflects the degree of deformation heterogeneity present. The scale term, or equivalently the constitutive heterogeneity term, can be used to interpret size effects in tension for smooth specimens. More details on wavelets, strain heterogeneities, gradients and scale-dependent constitutive equations are given below.

1.5. Gradients and wavelets

The wavelet transform is an integral transform developed in the 1980s in signal analysis to decompose complex and highly irregular signals into amplitudes depending on position and scale. It is now widely used in many fields of science and engineering but, surprisingly, its use in deformation problems has been rather limited. Nevertheless, wavelets is probably the most efficient mathematical tool to quantify deformation heterogeneity and patterning at various scales of observation. In fact, the wavelet transform may be thought of as a mathematical microscope, the spatial resolution of which may vary according to the "scale" chosen for the base functions (wavelets). The base functions are constructed from a single function, the "mother wavelet"; and the corresponding wavelet coefficients which are readily computed on the basis of it, provide local information on the function they are used to represent, as well as information on the scale (level of magnification). A large number of books have recently been written on the mathematical foundations of wavelets and related applications, but the treatise by Daubechies (1992) still remains a simple, elegant and self-contained mathematical treatment. The first authors who searched for applications of wavelet analysis to material mechanics problems seem to be Frantziskonis and Loret (1992). In particular, they used the shear band solution derived from the author's gradient theory (Aifantis, 1984b, 1987, 1992) to calibrate their analysis which was based on the wavelet representation of the δ-function to simulate the strain distribution in a shear band. In fact, Frantziskonis et al. (2001) have further elaborated on the idea of combining gradient theory and wavelet analysis to derive scale-dependent constitutive equations which, in turn, were used to interpret size effects in brittle materials. These results were favorably compared with Carpinteri's multifractal approach to size effects, as illustrated in a recent article by Konstantinidis et al. (2001). In fact, Konstantinidis (2000) used wavelets and neural networks to analyze atomic force microscope (AFM) data recently obtained by Engelke and Neuhauser (1995) and Brinck et al. (1998) for slip band clustering in single crystals and a specific example will be discussed here. It seems that it may be possible now to derive slip patterning profiles at resolutions higher than those allowed experimentally, by properly "training" a neural network on the basis of the available wavelet analyzed experimental data. In accordance with these developments, it will be shown in the present paper that a wavelet representation of the Aifantis–Serrin type shear band solution (Aifantis, 1984b) of gradient theory can lead to the derivation of scale-dependent constitutive equations which do not depend explicitly on strain gradients; and, therefore, extra gradient coefficients and higher order boundary conditions commonly required in the formulation of related boundary value problems are no longer necessary. Instead, a scale factor of a universal character also reflecting a dependence on the ratio of the "internal" over the "gage" lengths enters now into the constitutive equation which is thus

becoming scale-dependent. The ability of such scale-dependent constitutive equations to explain size effects (including those observed in tension) and successfully interpret related experimental observations at the micron scale, will be briefly discussed again in a subsequent section and further elaborated upon in the future (see also Konstantinidis, 2000).

2. Basic mathematical structure

2.1. Gradient elasticity

A rather general, yet simple enough, extension of classical elasticity theory reads

$$(1 - c_1 \nabla^2)\boldsymbol{\sigma} = (1 - c_2 \nabla^2)[\lambda(\operatorname{tr}\boldsymbol{\varepsilon})\,\mathbf{1} + 2\mu\boldsymbol{\varepsilon}], \qquad (2.1)$$

where $(\boldsymbol{\sigma}, \boldsymbol{\varepsilon})$ denote the stress and strain tensors, (λ, μ) are the classical Lamé constants, and (c_1, c_2) are the newly introduced gradient coefficients. This gradient elasticity model includes the Laplacian of the stress term $c_1 \nabla^2 \boldsymbol{\sigma}$ in addition to the Laplacian of the strain term in the right hand side of Eq. (2.1). In fact, the stress gradient term was added in order to dispense with the well-known stress singularity in dislocation and crack problems. In the absence of the stress gradient term ($c_1 \equiv 0$), the corresponding strain gradient elasticity model was shown (Altan and Aifantis, 1992, 1997; Ru and Aifantis, 1993; Unger and Aifantis, 1995, 2000; Gutkin and Aifantis, 1996, 1999a) to eliminate the strain singularity, but not the stress singularity, from these problems. Along the lines of the procedure outlined in Ru and Aifantis (1993), it can be shown that it is possible to obtain the solutions $(\mathbf{u}, \boldsymbol{\sigma})$ of boundary value problems based on Eq. (2.1) in terms of corresponding solutions of classical elasticity $(\mathbf{u}^0, \boldsymbol{\sigma}^0)$ through the inhomogeneous Helmholtz equations

$$(1 - c_2 \nabla^2)\mathbf{u} = \mathbf{u}^0; \qquad (1 - c_1 \nabla^2)\boldsymbol{\sigma} = \boldsymbol{\sigma}^0, \qquad (2.2)$$

provided that proper care is taken for the extra (due to higher order terms) boundary conditions or conditions at infinity. For the dislocation problems considered here the extra boundary conditions required for the determination of the displacement $\mathbf{u}$ in Eq. (2.2)$_1$ are discussed, for ex-

ample, in Ru and Aifantis (1993), Gutkin and Aifantis (1996, 1999a). The stress field $\boldsymbol{\sigma}$ in Eq. (2.2)$_2$ is determined in terms of an appropriate stress function satisfying the standard equations of equilibrium and the corresponding traction boundary conditions (Ru and Aifantis, 1993). The conditions at infinity are taken such that the strain and stress field at infinity are the same for the classical and the gradient solutions. It is not within the scope of the present article to provide further comments on the well-posedeness of general boundary value problems based on Eq. (2.1), the nature and physical meaning of associated boundary conditions, as well as uniqueness properties and wave propagation studies. This task will be undertaken in a future publication where the relation of Eq. (2.1) to other gradient and nonlocal theories will be discussed. It simply suffices to state here that Eq. (2.1) may be obtained by an appropriate series expansion of nonlocal integral expressions for the average stress $\bar{\boldsymbol{\sigma}}$ and average strain $\bar{\boldsymbol{\varepsilon}}$ in terms of their local counterparts $(\boldsymbol{\sigma}, \boldsymbol{\varepsilon})$.

In order to illustrate the potential of the gradient elasticity theory embodied in Eq. (2.1), we consider a mixed dislocation line coinciding with the x_3-axis of a Cartesian coordinate system (x_1, x_2, x_3) and a Burgers vector $\mathbf{b} = b_1\mathbf{e}_1 + b_3\mathbf{e}_3$ designating the edge (b_1) and screw (b_3) components. The displacement field $\mathbf{u}^0$ then reads

$$\mathbf{u}^0 = \frac{b_1\mathbf{e}_1 + b_3\mathbf{e}_3}{2\pi} \left\{ \arctan\frac{x_2}{x_1} + \frac{\pi}{2}\operatorname{sign}(x_2) \right.$$
$$\times [1 - \operatorname{sign}(x_1)] \left\} + \frac{b_1}{4\pi(1-v)} \left\{ \frac{x_1 x_2}{r^2}\mathbf{e}_1 \right.$$
$$\left. - \left[(1 - 2v)\ln r + \frac{x_1^2}{r^2} \right]\mathbf{e}_2 \right\}, \qquad (2.3)$$

where v is the Poisson ratio and r is the radial coordinate defined, as usual, by $r^2 = x_1^2 + x_2^2$. (Strictly speaking, the term $\ln r$ in the brackets should be replaced by $\ln(r/C)$ where C is an arbitrary constant, in order to make this term dimensionless. Without loss of generality, we take the numerical value of the constant C equal to unity since the strains and stresses depend on the derivatives of the displacements and, thus, the actual value of C is immaterial.) The elastic strain field ε_{ij}^0 (in units of $1/[4\pi(1-v)]$) reads

$$\varepsilon_{11}^0 = -b_1 x_2[(1-2v)r^2 + 2x_1^2]/r^4;$$

$$\varepsilon_{22}^0 = -b_1 x_2[(1-2v)r^2 - 2x_1^2]/r^4,$$

$$\varepsilon_{12}^0 = b_1 x_1(x_1^2 - x_2^2)/r^4;$$

$$\varepsilon_{13}^0 = -b_3(1-v)x_2/r^2;$$

$$\varepsilon_{23}^0 = b_3(1-v)x_1/r^2, \tag{2.4}$$

and the elastic stress field σ_{ij}^0 (in units of $\mu/[2\pi(1-v)]$) reads

$$\sigma_{11}^0 = \varepsilon_{11}^0(v \equiv 0); \quad \sigma_{22}^0 = \varepsilon_{22}^0(v \equiv 0);$$

$$\sigma_{33}^0 = v(\sigma_{11}^0 + \sigma_{22}^0);$$

$$\sigma_{12}^0 = \varepsilon_{12}^0; \quad \sigma_{13}^0 = \varepsilon_{13}^0; \quad \sigma_{23}^0 = \varepsilon_{23}^0. \tag{2.5}$$

The corresponding elastic energy W^0 of the dislocation per unit dislocation length is

$$W^0 = \frac{\mu}{4\pi}\left(b_3^2 + \frac{b_1^2}{1-v}\right)\ln\frac{R}{r_0} \tag{2.6}$$

where R denotes the size of the solid and r_0 is a cut-off radius for the dislocation elastic field near the dislocation line. It is noted that the expressions (2.4) and (2.5) are singular at the dislocation line and that when $r_0 \to 0$, W^0 becomes also singular.

Let us now derive the corresponding dislocation fields within the theory of gradient elasticity described by Eq. (2.1). As already indicated, the solution can be obtained by solving separately Eqs. (2.2)$_1$ and (2.2)$_2$ with the aid of appropriate extra boundary conditions dictated by the Burger's circuit and the smoothness at infinity. The solution is obtained by using the Fourier transform method. Omitting intermediate calculations, the total displacement solution given by Eq. (2.2)$_1$ reads

$$\mathbf{u} = \mathbf{u}^0 - \frac{b_1}{4\pi(1-v)}$$

$$\times \{[2x_1 x_2 \mathbf{e}_1 + (x_2^2 - x_1^2)\mathbf{e}_2]r^2\Phi_2 + \mathbf{e}_2\Phi_0\}$$

$$+ \frac{b_1\mathbf{e}_1 + b_3\mathbf{e}_3}{2\pi}\text{sign}(x_2)\int_0^\infty \frac{s\sin(sx_1)}{(1/c_2) + s^2}$$

$$\times e^{-|x_2|\sqrt{(1/c_2)+s^2}}\,ds, \tag{2.7}$$

where $\mathbf{u}^0$ is given by Eq. (2.3), $\Phi_0 = (1-2v) \times K_0(r/\sqrt{c_2})$, $\Phi_2 = [2c_2/r^2 - K_2(r/\sqrt{c_2})]/r^4$, with $K_n(r/\sqrt{c_2})$ denoting modified Bessel function of the second kind and $n = 0, 1, \ldots$ designating the order of

this function. For the strains ε_{ij}, solution of an equation exactly in form like Eq. (2.2)$_1$, gives $\varepsilon_{ij} = \varepsilon_{ij}^0 + \varepsilon_{ij}^{gr}$ where ε_{ij}^0 are given by Eq. (2.4) and ε_{ij}^{gr} (in units of $1/[2\pi(1-v)]$) are given by

$$\varepsilon_{11}^{gr} = b_1 x_2[(x_2^2 - vr^2)\Phi_1 + (3x_1^2 - x_2^2)\Phi_2];$$

$$\varepsilon_{22}^{gr} = b_1 x_2[(x_1^2 - vr^2)\Phi_1 + (3x_2^2 - x_2^2)\Phi_2];$$

$$\varepsilon_{12}^{gr} = -b_1 x_1[x_2^2\Phi_1 + (x_1^2 - 3x_2^2)\Phi_2];$$

$$\varepsilon_{13}^{gr} = b_3(1-v)x_2 r^2\Phi_1/2;$$

$$\varepsilon_{23}^{gr} = -b_3(1-v)x_1 r^2\Phi_1/2, \tag{2.8}$$

where $\Phi_1 = K_1(r/\sqrt{c_2})/(\sqrt{c_2}r^3)$. For the stresses σ_{ij}, solution of Eq. (2.2)$_2$ gives $\sigma_{ij} = \sigma_{ij}^0 + \sigma_{ij}^{gr}$ where σ_{ij}^0 are given by Eq. (2.5) and σ_{ij}^{gr} (in units of $\mu/[2\pi(1-v)]$) are given by

$$\sigma_{11}^{gr} = \varepsilon_{11}^{gr}(v \equiv 0, c_2 \leftrightarrow c_1);$$

$$\sigma_{22}^{gr} = \varepsilon_{22}^{gr}(v \equiv 0, c_2 \leftrightarrow c_1);$$

$$\sigma_{33}^{gr} = v(\sigma_{11}^{gr} + \sigma_{22}^{gr}); \quad \sigma_{12}^{gr} = \varepsilon_{12}^{gr}(c_2 \leftrightarrow c_1);$$

$$\sigma_{13}^{gr} = \varepsilon_{13}^{gr}(c_2 \leftrightarrow c_1); \quad \sigma_{23}^{gr} = \varepsilon_{23}^{gr}(c_2 \leftrightarrow c_1). \tag{2.9}$$

The main feature of the solution given by Eqs. (2.7)–(2.9) is the absence of any singularities in the displacement, strain and stress fields. In fact, when $r \to 0$, we have, $K_0(r/\sqrt{c_k})|_{r\to0} \to -\gamma^E + \ln(2\sqrt{c_k}/r)$, $K_1(r/\sqrt{c_k}) \to \sqrt{c_k}/r$, $K_2(r/\sqrt{c_k}) \to 2c_k/r^2 - 1/2$, where $\gamma^E = 0.57721566\ldots$ is Euler's constant and $k = 1, 2$. Thus, u_2 is finite, $\varepsilon_{ij} \to 0$, $\sigma_{ij} \to 0$. Using Eq. (2.9), the elastic energy (or self-energy) of the dislocation within the gradient elasticity theory given by Eq. (2.2), may be identified with the work $W_s = (-1/2)\int_V \sigma_{32}\beta_{23}^{(cl)}\,dV$ (for a screw component) and $W_e = (-1/2)\int_V \sigma_{12}\beta_{21}^{(cl)}\,dV$ (for an edge component) done by the gradient-dependent dislocation stress field for producing the corresponding classical (for simplicity) plastic distortion $\beta_{2\alpha}^{(cl)} = (b_\alpha/2)\delta(x_2)[1 - \text{sign}(x_1)]; \; \alpha = 1, 3$. The final result reads

$$W = \frac{\mu}{4\pi(1-v)}\left\{\frac{b_1^2}{2} + [b_1^2 + (1-v)b_3^2]\right.$$

$$\left. \times \left(\gamma^E + \ln\frac{R}{2\sqrt{c_1}}\right)\right\}, \tag{2.10}$$

which is non-singular at the dislocation line. It is worth noting that the above expression contains only one gradient coefficient (c_1), since the clas-

sical part of the plastic distortion $\boldsymbol{\beta}^{(\mathrm{cl})}$ was used in the definition of the work or elastic energy. If $\boldsymbol{\beta}^{(\mathrm{gr})}$ is also included, e.g. $\beta_{23}^{(\mathrm{gr})} = (b_3/2)\delta(x_2)[1 - \mathrm{sign}(x_1)] \times (1 - \mathrm{e}^{-|x_1|/\sqrt{c_2}})$ for the screw component, then the expression $W_s = (1/2)\int_V \sigma_{32}\beta_{23}^{(\mathrm{gr})}\,\mathrm{d}V$ for the screw component would contain both c_1 and c_2. The same would be true for the edge component. It is noted, in this connection, that such different expressions for W are a result of the form of the work expression assumed. An alternative method for computing W is to introduce an appropriate strain energy function for the gradient elasticity theory at hand.

It may be instructive to specialize the above results for the case of a screw dislocation and the simplest possible gradient elasticity model resulting from Eq. (2.1) with $c_1 \equiv 0$ and $c_2 \equiv \bar{c}$ (Aifantis, 1992). The corresponding strain components read

$$\varepsilon_{13} = \frac{b}{4\pi}\left[-\frac{x_2}{r^2} + \frac{x_2}{r\sqrt{\bar{c}}}K_1\left(\frac{r}{\sqrt{\bar{c}}}\right)\right];$$

$$\varepsilon_{23} = \frac{b}{4\pi}\left[\frac{x_1}{r^2} - \frac{x_1}{r\sqrt{\bar{c}}}K_1\left(\frac{r}{\sqrt{\bar{c}}}\right)\right], \tag{2.11}$$

where b denotes the Burgers vector and r denotes, as before, the radial coordinate from the dislocation line. The first term in the bracket represents the singular classical elasticity solution and the second term with the Bessel function K_1 represents the gradient elasticity contribution. It is noted that $K_1(r/\sqrt{\bar{c}}) \to \sqrt{\bar{c}}/r$ as $r \to 0$ and, thus, the gradient term cancels the elastic singularity as the dislocation line is approached. It turns out that a dislocation core may be defined at $r \sim r_c = 1.25a$, and that the strain achieves extreme values at a location $\sim 12\%$ of this distance. The corresponding elastic energy W_s is governed by the term $(\mu b^2/4\pi)\ln[R/2\sqrt{\bar{c}}]$ which does not contain any cut-off radius usually assumed for the dislocation self-energy expression of the classical elasticity solution. Analogous expressions can be obtained for edge components, as well as disclinations and other dislocation arrangements. It is expected that the implications of these results may be important for the characterization of short-range interactions and the precise determination of stresses, strains and energies of defects controlling the behavior of

interfaces (misfit dislocations, threading dislocations) and nanocrystals (linear disclinations in triple-junctions and point disclinations in fourfold nodes of triple-junction lines). These solutions can also be used for deriving non-singular expressions for cracks by representing them by appropriate continuous distributions of dislocations, as well for characterizing the spatial details of the crack tip.

On returning to the more general case of Eq. (2.1) and the problem of evaluation of stresses for a screw dislocation (along the axis x_3) sitting at a flat interface (coinciding with the plane $x_1 = 0$) separating two infinitely extended media with elastic constants (λ_1, μ_1) and (λ_2, μ_2), it is noted that this task is reduced to the solution of Eq. (2.2)$_2$ where, for simplicity, we assume that the gradient coefficients $c_1^{(1)} = c_1^{(2)} \equiv c^*$. The corresponding interfacial conditions read

$$[\sigma_{13}]_{x_1=0} = 0; \quad [\sigma_{23}]_{x_1=0} = 0; \quad \left[\frac{\partial\sigma_{\alpha3}}{\partial x_1}\right]_{x_1=0} = 0$$

$$\text{with } \alpha = 1, 2. \tag{2.12}$$

The first condition is the same as in the classical theory of elasticity, while the last three are extra conditions associated with the gradient term; the symbol [ ] denotes, as usual, the jump across the interface (Ru and Aifantis, 1993). The corresponding stresses σ_{ij} (in units $\mu_1\mu_2 b/\pi[\mu_1 + \mu_2]$) read

$$\sigma_{13} = -\frac{x_2}{r^2} + \frac{x_2}{r\sqrt{c^*}}K_1\left(\frac{r}{\sqrt{c^*}}\right);$$

$$\sigma_{23} = \frac{x_1}{r^2} - \frac{x_1}{r\sqrt{c^*}}K_1\left(\frac{r}{\sqrt{c^*}}\right), \tag{2.13}$$

and the resemblance with the expressions given by Eq. (2.11) is obvious. In fact, these expressions are identical in form (they differ only by the factor $2\mu_2/[\mu_1 + \mu_2]$) to those obtained for a screw dislocation in an infinite homogeneous gradient elastic medium governed by Eq. (2.1). If the dislocation lies at a position $x_1 = x^*$ from the interface within the medium with elastic constants (λ_1, μ_1), the image force F^{im} which acts upon the dislocation unit length due to the interface (in units $\mu_1 b^2/2\pi$) reads

$$F^{\mathrm{im}}(x^*) = -\frac{\mu_1 - \mu_2}{\mu_1 + \mu_2}\left[\frac{1}{2x^*} - \int_0^\infty e^{-x^*(\lambda^* + s)}\,\mathrm{d}s\right];$$
$$\lambda^* \equiv \sqrt{(1/c^*) + s^2}, \tag{2.14}$$

where the first term in the brackets is the classical singular solution and the second one is the extra gradient term. The numerical evaluation of Eq. (2.14) shows that the classical singularity is eliminated from the gradient solution which attains a maximum at a distance $\cong \sqrt{c^*}$ from the interface and tends to zero at the interface.

2.2. Gradient defect kinetics

Beyond elastic deformation, the production/annihilation and motion of defects dictate the evolution of deformation field. In general, various families of defects may be identified depending on the deformation mechanism at hand. A general starting point then would be a set of equations of the form

$$\frac{\partial \rho_k}{\partial t} + \mathrm{div}\,\mathbf{J}_k = F_k(\{\rho_i\});$$
$$\mathbf{J}_k = \rho_k \mathbf{v}_k - D_k \nabla \rho_k, \tag{2.15}$$

which accounts for defect production/annihilation in terms of the source terms F_k (where the symbol $\{\rho_i\}$ denotes dependence on all defect populations ρ_i) and motion in terms of the defect fluxes $\mathbf{J}_k$. The first term of Eq. $(2.15)_2$ describes the deterministic motion of defects of density ρ_k with velocity $\mathbf{v}_k$ (e.g. dislocations moving under the influence of an applied stress), while the "diffusion coefficient" D_k accounts for random influences on the motion of these defects. In different physical situations, different mechanisms leading to diffusion-like terms may be envisaged. The density ρ_k may refer to positive or negative dislocations, mobile dislocations or immobile dipoles, misfit or threading dislocations, disclinations or disclination dipoles and other type of possible defects depending on the physical situation and the desired degree of detail for the material description at hand. A stochastic generalization of Eq. (2.15) is given by the Langevin-type equation

$$\frac{\partial \rho_k}{\partial t} + \mathrm{div}\,\mathbf{J}_k = F_k(\{\rho_i\}) + G_k(\{\rho_i\})\dot{w}_k \tag{2.16}$$

In this stochastic differential equation, the evolution of the dislocation densities is influenced by additional stochastic terms $G_k \dot{w}_k$ where $\dot{w}_k$ are random processes. These terms may, in principle, account for any random influences on the defect dynamics.

In the work of Hahner (1996a,b) the stochastic character of microstructural evolution was related to the large intrinsic fluctuations of the dislocation velocity (or the local rate of slip) that arise due to the collective nature of dislocation glide. These fluctuations manifest themselves through the formation of slip lines or slip bands. In fact, it is the competition of the deterministic gradient terms $D_k \nabla^2 \rho_k$ and the stochastic terms $G_k \dot{w}$ that determines the inhomogeneous evolution of the ensemble of defects and associated deformation localization phenomena. Certain deformation patterning phenomena (such as PSBs and Lüders bands, but not slip lines in stage I/II hardening of FCC metals) can also be conveniently interpreted within a strictly deterministic framework on the basis of Eq. (2.15) as illustrated earlier by the author and his co-workers (e.g. Aifantis, 1999a,b; Bammann and Aifantis, 1982; Walgraef and Aifantis, 1985; Romanov and Aifantis, 1993; Liosatos et al., 1998; Cholevas et al., 1998; Aifantis, 1987, 1992, 1995, 1996). A framework based on Eq. (2.15) may also be used effectively for describing the deformation of nanocrystals. A multi-element gradient defect kinetics model involving four populations of defects with densities $\rho_1 = \rho$ (intragrain mobile dislocations), $\rho_2 = \varphi$ (intragrain mobile dislocation dipoles), $\rho_3 = \psi$ (grain boundary sliding dislocations) and $\rho_4 = \vartheta$ (grain boundary junction disclinations) can be employed for this purpose. Stability analysis of the corresponding system of reaction-diffusion type equations can then provide insight into the grain size regime where solutions for ρ and φ are not stable. This may elucidate the mechanisms of plastic deformation at the nanoscale; in particular, the grain size regime where a plasticity transition occurs from a grain rotation/sliding mechanism in the absence of intragrain dislocation activity to a massive intragrain dislocation motion which is the traditional mechanism of plastic deformation for conventional polycrystals.

In concluding this section on gradient defect kinetics, it is pointed out that it is possible (under certain assumptions) to derive from Eq. (2.15) for the evolution of defect density an equation for the evolution of the local plastic strain. Then, within a one-dimensional framework, this evolution equation for the plastic strain γ (with α denoting a viscoplastic-like coefficient and c being a gradient coefficient) reads

$$\alpha \frac{\partial \gamma}{\partial t} = \sigma_{\text{ext}} - \bar{\sigma}_{\text{int}}(\gamma) - \delta\sigma_{\text{int}}(\gamma, x) + c \frac{\partial^2 \gamma}{\partial x^2};$$

$$\langle \delta\sigma_{\text{int}}(\gamma, x) \delta\sigma_{\text{int}}(\gamma', x') \rangle$$

$$= \langle (\delta\sigma_{\text{int}})^2 \rangle f\left(\frac{x - x'}{\xi}\right) g\left(\frac{\gamma - \gamma'}{\gamma_{\text{corr}}}\right), \qquad (2.17)$$

where σ_{ext} is the external stress, σ_{int} is the internal stress with mean value $\bar{\sigma}_{\text{int}}$ and fluctuations $\delta\sigma_{\text{int}}$ obeying Eq. $(2.17)_2$. (The mean internal stress accounts for both the conventional flow stress and for long-range stresses that arise from large-scale incompatibilities of slip. Thus, its general form may be written as $\bar{\sigma}_{\text{int}}(\gamma) = \sigma_f(\gamma) - \int \gamma(r') \Gamma(r - r') \mathrm{d}^3 r'$, where the first term describes how the local interactions between defects oppose plastic flow, while the second term is a long-range stress which can be expressed as the convolution of the plastic strain with certain Green's function.) The term $\langle (\delta\sigma_{\text{int}})^2 \rangle$ defines the amplitude of stress variations, γ_{corr} is the characteristic strain interval over which such fluctuations persist, and ξ is the characteristic range over which $\delta\sigma_{\text{int}}(\gamma, x)$ changes in space. (The functions f and g are normalized such that $f(0) = g(0) = 1$ and $\int f(s) \mathrm{d}s = \int g(s) \mathrm{d}s = 1$.) For a tensile specimen of length L in the absence of the gradient term, the local strain rate fluctuates in general and in large systems the average fluctuations decrease like $L^{1/2}$. The effect of the gradient term is to induce a stress redistribution by decreasing deformation resistance in the vicinity of increased strain regions. The result is an avalanche dynamics, as detailed in a forthcoming article by Zaiser and Aifantis (in press). For strain softening solids, a quasi-static version of Eq. (2.17), with its first term set equal to zero, can be employed to model the slip patterning during straining of a single crystal and the associated serrations in the corresponding stress–strain graph. In this case,
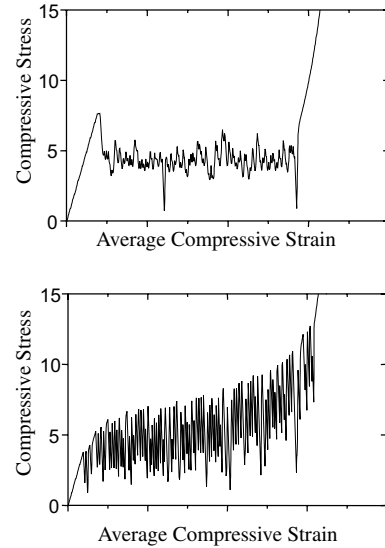

Fig. 1. Serrated stress–strain graphs as a result of the competition between gradient and stochastic terms.

$\bar{\sigma}_{\text{int}}(\gamma)$ is assumed to be of an N-shaped form, the orientation factor relating the uniaxial stress to the critical resolved stress is formally set equal to unity (since it is a constant factor, entering simply in the equation as a scalar multiplier), and the effect of randomness is taken simply by multiplying $\bar{\sigma}_{\text{int}}$ with the factor $[1 + w(x)]$, where $w(x)$ denotes a random function of x. Then a cellular automaton treatment based on the resulting equation, can lead to the serrated stress–strain graphs depicted in Fig. 1. These graphs are qualitatively similar to those obtained by Zaiser and Aifantis (in press) for the crushing of cellular solids subjected to compression. The top graph corresponds to small randomness and strong spatial couplings, while the bottom graph corresponds to large randomness and weak spatial couplings. Further details will be reported by Zaiser and Aifantis (in press) and in a forthcoming publication. It will further be substantiated there, through the use of cellular automata (based on a discrete analogue of Eq. (2.12)) and actual numerical simulations (based on the numerical solution of Eq. (2.17)), that Eq. (2.17) with a strain hardening/softening law can be applied to both strain softening in single crystals (e.g. Lüders bands with randomness) and to strain softening in cellular solids.

2.3. Gradient plasticity

The above discussion on the deduction of gradient type evolution equations for the plastic strain on the basis of corresponding equations for defect densities, may be used as a direct motivation for a phenomenological theory of gradient plasticity as detailed below.

Within a deformation version of such theory, the following relation between effective stress $\tau \equiv \sqrt{1/2\sigma'_{ij}\sigma'_{ij}}$ and effective strain $\gamma \equiv \sqrt{2\varepsilon'_{ij}\varepsilon'_{ij}}$ (σ'_{ij} denotes the deviatoric part of the stress tensor σ_{ij}; ε'_{ij} denotes the deviatoric part of the strain tensor ε_{ij} with $\varepsilon_{kk} = 0$ and, thus, $\varepsilon'_{ij} = \varepsilon_{ij}$)

$$\tau = \kappa(\gamma) + c_1(\gamma)|\nabla\gamma|^m + c_2(\gamma)\nabla^2\gamma, \qquad (2.18)$$

can be used as a starting point. The function $\kappa(\gamma)$ denotes the usual homogeneous part of the flow stress, while $c_1(\gamma)$ and $c_2(\gamma)$ are the newly introduced gradient coefficients which, in general, depend on the equivalent strain γ. Using the equivalent plastic work relation $\sigma'_{ij}\delta\varepsilon_{ij} = \tau\delta\gamma$, the following gradient dependent stress–strain relation is derived

$$\sigma'_{ij} = \frac{2}{\gamma}\left[\kappa(\gamma) + c_1(\gamma)|\nabla\gamma|^m + c_2(\gamma)\nabla^2\gamma\right]\varepsilon_{ij}. \qquad (2.19)$$

On denoting by $(\mathbf{t},\mathbf{u})$ the traction and displacement vectors respectively, numerical solutions can be obtained on the basis of the relation $\int_V \sigma_{ij,j}\delta u_i\,\mathrm{d}V = 0$ implying, with the aid of the divergence theorem, the condition

$$\int_{\partial V} t \cdot \delta\mathbf{u} = \int_V \{[\kappa(\gamma) + c_1|\nabla\gamma|^m - c'_2|\nabla\gamma|^2]\delta\gamma$$
$$- c_2(\nabla\gamma \cdot \nabla\delta\gamma)\}\,\mathrm{d}V = 0, \qquad (2.20)$$

where here and subsequently a prime on a material function depending on γ denotes differentiation with respect to γ, e.g. $c'_2 = \mathrm{d}c_2/\mathrm{d}\gamma$, and the extra boundary conditions $d\gamma = 0$ or $\nabla\gamma \cdot \mathbf{n} = 0$ with $\mathbf{n}$ denoting the outward unit normal to the boundary ∂V, were utilized. The above equation can be solved, for example, with the aid of the finite element method by discretizing only the displacement $\mathbf{u}$, in terms of which the rest of the quantities in Eq. (2.20) can be expressed.

Along similar lines, a flow version of gradient plasticity theory can be formulated. The appropriate yield condition now reads

$$F = \tau - [\kappa(\gamma) + c_1(\gamma)|\nabla\gamma|^m - c'_2(\gamma)|\nabla\gamma|^2] = 0, \qquad (2.21)$$

where the equivalent strain γ is now defined in terms of the plastic strain tensor $\dot{\varepsilon}^p_{ij}$ as $\gamma = \int \dot{\gamma}\mathrm{d}t$, $\dot{\gamma} \equiv \sqrt{2\dot{\varepsilon}^p_{ij}\dot{\varepsilon}^p_{ij}}(\dot{\varepsilon}^p_{kk} = 0)$. The corresponding flow rule reads

$$\dot{\varepsilon}^p_{ij} = \dot{\gamma}\frac{\partial F}{\partial\sigma_{ij}} \Rightarrow \dot{\varepsilon}^p_{ij} = \frac{\dot{\gamma}}{2\tau}\sigma'_{ij}. \qquad (2.22)$$

The elastic strain increment $\dot{\varepsilon}^e_{k\ell} = \dot{\varepsilon}_{k\ell} - \dot{\varepsilon}^p_{k\ell}$ is determined by Hooke's law which may be written in the form $\dot{\sigma}_{ij} = C^e_{ijk\ell}(\dot{\varepsilon}_{k\ell} - \dot{\varepsilon}^p_{k\ell})$; $C^e_{ijk\ell} = \lambda\delta_{ij}\delta_{k\ell} + \mu(\delta_{ik}\delta_{j\ell} + \delta_{i\ell}\delta_{jk})$, with ε_{ij} being the total strain tensor and (λ, μ) denoting the Lamé constants of an isotropic elastic material.

The "plastic multiplier" $\dot{\gamma}$ in the flow rule given by Eq. (2.22) satisfies the following loading–unloading conditions

$$\dot{\gamma} = \begin{cases} \dot{\gamma} & \text{if } F = 0 \text{ \& } \sigma_{ij}\dot{\varepsilon}^p_{ij} > 0 \text{ (loading) or} \\ & \quad \sigma_{ij}\dot{\varepsilon}^p_{ij} = 0 \text{ (neutral loading)}, \\ 0 & \text{if } F < 0 \text{ (elasticity) or } F = 0 \text{ and} \\ & \quad \sigma_{ij}\dot{\varepsilon}^p_{ij} < 0 \text{ (unlodging)}, \end{cases} \qquad (2.23)$$

and is determined by the consistency condition $\dot{F} = 0$, which along with Hooke's law leads to the following differential equation for the determination of the plastic multiplier $\dot{\gamma}$

$$\dot{\gamma} + m\frac{c_1}{H}|\nabla\gamma|^{m-2}(\nabla\gamma \cdot \nabla\dot{\gamma}) + \frac{c_2}{H}\nabla^2\dot{\gamma}$$
$$= \frac{1}{H}\frac{\sigma'_{ij}}{2\tau}C^e_{ijkl}\dot{\varepsilon}_{kl}, \qquad (2.24)$$

where $H \equiv h_g + (\sigma'_{ij}C^e_{ijkl}\sigma'_{kl}/4\tau^2) = h_g + 3\mu$; $h_g = \kappa'(\gamma) + c'_1(\gamma)|\nabla\gamma|^m + c'_2(\gamma)\nabla^2\gamma$. This, i.e. Eq. (2.24), is a notable departure of the gradient plasticity theory from the classical theory where $\dot{\gamma}$ is determined from an algebraic equation. Numerical solution of boundary value problems can now be

established by utilizing the weak satisfaction of stress equilibrium in rate form, i.e.

$$
\begin{aligned}
\int_V (\dot{\sigma}_{ij,j})\delta\dot{u}_i\,\mathrm{d}V = 0 &\Rightarrow \int_V \dot{\sigma}_{ij}\delta\dot{\varepsilon}_{ij}\,\mathrm{d}V \\
&= \int_{\partial V} \dot{t}_i\delta\dot{u}_i\,\mathrm{d}S \\
&= \int_V \left(C^{\mathrm{e}}_{ijkl}\dot{\varepsilon}_{kl} - \frac{\mu\sigma'_{ij}}{\tau}\dot{\gamma} \right)\delta\dot{\varepsilon}_{ij}\,\mathrm{d}V,
\end{aligned}
\tag{2.25}
$$

where the last equality of Eq. (2.25) is established with the aid of Hooke's law and the flow rule. The weak satisfaction of the consistency condition implies

$$
\int_{V_{\mathrm{p}}} \left[\frac{\sigma'_{ij}}{2\tau}C^{\mathrm{e}}_{ijkl}\dot{\varepsilon}_{kl} - H\dot{\gamma} \right. \\
\left. - mc_1|\nabla\gamma|^{m-2}(\nabla\gamma\cdot\nabla\dot{\gamma}) - c_1\nabla^2\dot{\gamma} \right]\delta\dot{\gamma}\,\mathrm{d}V = 0.
\tag{2.26}
$$

Integration by parts in the last term yields

$$
\begin{aligned}
\int_{V_{\mathrm{p}}} (c_2\nabla^2\dot{\gamma})\delta\dot{\gamma}\,\mathrm{d}V = &\int_{\partial V_{\mathrm{p}}} (c_2\nabla^2\dot{\gamma}\cdot\mathbf{n})\delta\dot{\gamma}\mathrm{d}S \\
&- \int_{V_{\mathrm{p}}} c_2(\nabla\dot{\gamma}\cdot\nabla\dot{\gamma})\,\mathrm{d}V \\
&- \int_{V_{\mathrm{p}}} c'_2(\nabla\gamma\cdot\nabla\dot{\gamma})\delta\dot{\gamma}\,\mathrm{d}V, \quad (2.27)
\end{aligned}
$$

which suggests the form of the extra boundary conditions, i.e. $\nabla^2\dot{\gamma}\cdot\mathbf{n} = 0$ or $\delta\dot{\gamma} = 0$ on ∂V_{p}. Eqs. (2.26) and (2.27) can then be solved simultaneously by discretizing both γ and $\mathbf{u}$ fields.

3. The phenomenological gradient coefficients and the origin of gradient terms

The simplest possible form of gradient theory is described by the following equations for the scalar dislocation density ρ, the equivalent plastic shear strain γ and the elastic strain ε_{ij}

$$
\partial\rho/\partial t = D\nabla^2\rho + f(\rho),
\tag{3.1}
$$

$$
\tau = \kappa(\gamma) - c\nabla^2\gamma,
\tag{3.2}
$$

$$
\sigma_{ij} = \lambda\varepsilon_{kk}\delta_{ij} + 2\mu\varepsilon_{ij} - \bar{c}\nabla^2(\lambda\varepsilon_{kk}\delta_{ij} + 2\mu\varepsilon_{ij}).
\tag{3.3}
$$

The gradient coefficients D in Eq. (3.1), c in Eq. (3.2) and $\bar{c}$ in Eq. (3.3) denote gradient phenomenological coefficients the value of which is to be determined from appropriate experiments, as well as appropriate microscopic arguments depending on the prevailing deformation mechanisms and the underlying microstructure. The strain rate and temperature dependence have been suppressed in Eqs. (3.1)–(3.3) for convenience. Such dependence is particularly important in problems of creep and recrystallization, as well as for dynamic shear banding and strain-rate dependent materials.

As already mentioned, gradient-dependent expressions of the type of Eqs. (3.1)–(3.3) have been successfully employed to predict dislocation patterning phenomena, shear band widths and spacings, as well as to eliminate strain singularities from dislocation lines and elastic crack tips (e.g. Aifantis (1999a,b)). The value of the gradient coefficients can be estimated from such dislocation pattern wavelengths and shear band widths measurements, as well as from possible experiments at the atomic scale pertaining to the extent of dislocation cores and the structure of crack tip opening profiles. Direct estimates for the gradient coefficients can also be obtained from properly designed experiments, as discussed below.

3.1. The phenomenological gradient coefficients

3.1.1. Gradient plasticity

Pure bending experiments of asymmetrically deforming beams (due to an inhomogeneous engineered microstructure—e.g. grain size distribution along the beam axis) can provide estimates of the gradient coefficient c in Eq. (3.2). Preliminary results have already been obtained and a brief outline of this possibility has been reviewed by the author (Aifantis, 1992; Aifantis, 1995). The aforementioned experimental estimates for the gradient coefficient of deformed polycrystals seem to be in good agreement with theoretical estimates obtained by using self-consistent arguments as discussed also in (Aifantis, 1995). The self-consistent estimate for the gradient coefficient c gives the expression $|c| = (\beta + h)(d^2/10)$, where β relates

explicitly to the elastic constants of the material in a fashion depending on the self-consistent model used, while h is the plastic hardening modulus. The parameter d stands for the grain size. The self-consistent method or an improved averaging procedure may be employed to consider different than polycrystalline situations; for example, a continuous distribution of dislocations, a continuous distribution of flat cracks, a continuous distribution of spherical voids, etc. In each case a different expression for the gradient coefficient c would result depending on the geometric characteristics of the underlying microstructure and the associated internal lengths (e.g. void size and spacing).

3.1.2. Gradient dislocation dynamics

Similarly, for the diffusion-like coefficient D, various dislocation mechanisms can be considered to derive appropriate microscopic relations for it. They all lead to an expression of the form $D = \bar{\ell}\langle v \rangle$, where $\bar{\ell}$ denotes a mean free path and $\langle v \rangle$ the average dislocation velocity. For instance, one may consider the motion of one particular dislocation which, in addition to the external stress, is influenced by the long-range stress field of the ensemble of all other dislocations. In a first approximation, this influence may be accounted for in terms of random effective stress fluctuations $\delta\tau_{\text{eff}}$ which act on the dislocation and lead to random fluctuations of the dislocation velocity. This argument leads to the expression $\bar{\ell} \sim \langle \delta\tau_{\text{eff}}^2 \rangle \ell_{\text{corr}}/S^2$, where $\langle \delta\tau_{\text{eff}}^2 \rangle$ stands for the amplitude of the effective stress fluctuations, ℓ_{corr} denotes the corresponding correlation length and S is the strain rate sensitivity. If a cross-slip mechanism is assumed, then it turns out that $\bar{\ell} = (\bar{h}^2/\ell_s)[1 + 2(h_0/\bar{h})^2 + 1/2(h_0/\bar{h})]\exp(-h_0/\bar{h})$, where ℓ_s denotes an average distance between cross-slip events, h_0 denotes the distance of dislocation immobilization for dipole formation ($h_0 = \mu b/2\pi(1-v)(\tau - \tau_f)$; μ is the shear modulus, b is the Burgers vector, v is the Poisson's ratio, τ is the resolved shear stress and τ_f is the friction stress), and $\bar{h} = \int hP(h)\,dh$ with $P(h)$ denoting the probability for the cross-slip height to be h. For a polycrystalline situation and an elementary volume containing a large number of grains and slip systems with gliding dislocations, it turns out that

$\bar{\ell} = d\langle \tan^2 \varphi \rangle/4$ where d denotes the grain size and $\langle \tan^2 \varphi \rangle$ is a numerical factor resulting from the averaging of all gliding and grain orientations. If we distinguish between positive and negative mobile dislocations, write standard dislocation dynamics evolution equations for both populations (without including diffusion-like coefficients at the outset, but accounting for their flux within the elementary volume (Aifantis, 1984c, 1987, 1992)), and then adiabatically eliminate the "fast variable" of their difference for cases that this is physically justified, we obtain a diffusion term in the corresponding evolution equation for the sum or total mobile dislocation density which is now of the form of Eq. (3.1). The internal length $\bar{\ell}$ turns out to be of the form $\bar{\ell} = vt_{\text{life}}$ where v denotes the mobile dislocation velocity and t_{life} is the mean lifetime of mobile dislocations which, in general, depends on the densities of all other defects. Finally, if a "dipole exchange" mechanism is considered as proposed by Differt and Essmann, a relation of the form of Eq. (3.1) can be written for an "immobile" population of dislocation dipoles. Then, the appropriate expression for the dislocation diffusivity reads $D \approx y_d^2/8t_d = \rho_m v y_d^3/4$ where y_d is the mean dipole height and t_d^{-1} is the rate of the dipole exchange interaction, while ρ_m and v denote as usual the density and velocity of the mobile dislocations. An evolution equation of the form of Eq. (3.1) for the density of immobile dislocations may also be deduced by considering the coupling of immobile dislocations with point defects. Adiabatic elimination of the point defect density would lead then to a diffusion-like term for immobile dislocations with a diffusivity depending on the diffusion coefficient and the production/annihilation reaction constants of point defects. (In the simplest case, D in Eq. (3.1) would be directly proportional to the diffusivity of point defects.) Related considerations of such type of dislocation mechanisms arguments can be found in a recent article by Zaiser and Aifantis (1999).

A more deductive derivation of gradient or diffusion-like terms in the equations of dislocation dynamics is possible by starting with the equation of motion for each discrete dislocation in a single slip configuration, i.e.

$$(1/M)v_i = \tau_{\text{ext}} + \int \tau(\mathbf{r} - \mathbf{r}')[\rho_d^+(\mathbf{r}') - \rho_d^-(r')]\, \mathrm{d}^2 r';$$

$$\rho_d^\pm = \sum_{i \neq j^{(\pm)}} \delta(\mathbf{r}' - r_j), \tag{3.4}$$

where M denotes a mobility-like coefficient, v_i is the velocity of the ith dislocation, $\rho_d^\pm$ is the discrete density of positive or negative dislocations, the δ denote δ-functions introduced to account for the discreteness of the dislocation configuration assumed, τ_{ext} is the external resolved shear stress and $\tau(\mathbf{r} - \mathbf{r}')$ is an elastic kernel determined by classical elasticity depending on the type of dislocations considered. Averaging of the above discrete equations of dislocation dynamics over an ensemble of statistically equivalent dislocation populations $[\rho^\pm(\mathbf{r}') \equiv \langle \rho_d^\pm(\mathbf{r}') \rangle, v(\mathbf{r}) \equiv \langle v_i \rangle]$ yields the equation of motion

$$(1/M)v(\mathbf{r}) = \tau_{\text{ext}} + \int \tau(\mathbf{r} - \mathbf{r}')\{\rho^+(\mathbf{r}')[1 + d^{++}(\mathbf{r} - \mathbf{r}')]$$
$$- \rho^-(\mathbf{r}')[1 + d^\pm(\mathbf{r} - \mathbf{r}')]\}\, \mathrm{d}^2 r', \tag{3.5}$$

where the first term in the bracket $\{\ \}$ under the integral designates the probability to find a positive dislocation within $\mathrm{d}^2 r'$ around $\mathbf{r}'$ when there is a positive dislocation at $\mathbf{r}$; the second term designates the same for a negative dislocation at $\mathbf{r}'$. The symbols $(d^{++}, d^\pm)$ designate correlation functions (for a random dislocation arrangement $d^{++} = d^\pm = 0$) satisfying the following symmetry conditions $d^{++}(\mathbf{r}) = d^{++}(-\mathbf{r})[\equiv d^{--}(\pm \mathbf{r})], d^\pm(\mathbf{r}) = -d^{-+}(-\mathbf{r})$, as well as the scaling properties $d^{++} = d^{++}(\mathbf{r}\sqrt{\rho}), d^\pm(\mathbf{r}\sqrt{\rho})$ implied from standard dislocation dynamics arguments. (The starting point of Eq. (3.4) has been adopted in unpublished work by the author and Romanov, but the subsequent arguments based on the use of correlation functions and their properties were motivated by the work of Groma as elaborated upon recently by Zaiser and the details will be contained in a joint forthcoming report by these three authors.) It further turns out that the correlation functions $(d^{++}, d^\pm)$ decay faster than algebraically at large and, thus, a Taylor expansion approximation under the integral sign in Eq. (3.5) is justifiable. In fact, by considering the evolution equation or effective mass balance (Aifantis, 1987) for the positive dislocation density

population ρ^+ in one dimension (v^+ denotes velocity and C^+ production/annihilation) of the form

$$\frac{\partial \rho^+}{\partial t} + \nabla_x(\rho^+ v^+) = C^+, \tag{3.6}$$

and a similar equation can be written for the evolution of the negative dislocation population ρ^-. By adopting the aforementioned Taylor expansion approximation for the velocity v^+ in Eqs. (3.5) and (3.6) is written as

$$\frac{\partial \rho^+}{\partial t} + \nabla_x(\rho^+ \bar{v}) = D^+ \nabla_{xx}^2 \rho^+ + C^+, \tag{3.7}$$

and a similar equation can be written for ρ^-. The diffusion-like coefficient D^+ turns out to be of the form $D^+ = \beta \mu b M(\rho^+/\rho)$ with β denoting the value of an explicitly calculated integral, μ is the shear modulus, b is the Burgers vector, and ρ is the total dislocation density. The quantity $\bar{v}$ denotes what is commonly known in standard dislocation dynamics considerations as the average dislocation velocity which is now explicitly calculated on the basis of Eq. (3.5) and given by the expression $\bar{v} = M(\tau_{\text{ext}} + \tau_{\text{LR}} - \tau_{\text{back}})$, where $\tau_{\text{LR}} \equiv \int \tau(\mathbf{r} - \mathbf{r}') \times [\rho^+(\mathbf{r}')\rho^-(\mathbf{r}')]\, \mathrm{d}r'$ and $\tau_{\text{back}} = (\rho^-/\rho)\alpha \mu b \sqrt{\rho}$ denote the dislocation long-range stress and back stress respectively, with α being the standard numerical factor used in previously proposed expressions for the back stress. A similar equation like Eq. (3.7) holds for the negative dislocation density ρ^- and further details will be provided in a complete future treatment of the subject.

3.1.3. Gradient elasticity

Atomistic and/or homogenization techniques can be employed to derive microscopic expressions for the phenomenological coefficient $\bar{c}$ of the gradient elasticity model described by Eq. (3.3). Such expressions can be deduced, for example, from the work of Triantafyllidis and Aifantis (1986) based on atomistic considerations or the more recent work of Fish and Belsky (1995), and Fish et al. (2002) based on homogenization techniques. Along the same lines, expressions for the coefficient $\bar{c}$ may be deduced from the nonlocal elasticity kernel recently derived by Picu (2002) to revisit the Peierls–Nabarro model and calculate the

corresponding Peierls stress. In fact, the gradient elasticity model given by Eq. (3.3) may also be viewed (but not necessarily) as a Taylor approximation of a non-local elasticity model of the form $\sigma_{ij} = \int_v \alpha(|\mathbf{r} - \mathbf{r}'|)\sigma_{ij}^c(\mathbf{r}')d^3\mathbf{r}$ where $\mathbf{r}$ denotes the spatial polar coordinate σ_{ij}^c and is the classical stress given by Hooke's law. A commonly used form for the non-local elasticity kernel is $\alpha(|\mathbf{r} - \mathbf{r}'|) = \alpha_0 \times \exp[-(\mathbf{r} - \mathbf{r}'/mb^2]$ where $\alpha_0 = 1/\pi\sqrt{\pi}m^3$ with mb denoting an internal length scale and b is the Burgers vector. The newly proposed form by Picu (2002) in one dimension reads $\alpha(x) = \alpha_0\{[1 - (x/n)^{2k_1} \times \exp[-(x/m)^{2k_2}]\}$, where all constants are material lattice parameters. The implications of this new kernel to gradient elasticity models and related applications will be discussed elsewhere (Picu, 2002). Finally, it is pointed out that expressions for the gradient coefficient $\bar{c}$ can also be obtained by comparing the dispersive wave propagation relation resulting from gradient elasticity with the classical dispersion relation of lattice dynamics in the Brillouin regime. This gives $\sqrt{\bar{c}} \cong a/4$, where a designates the usual lattice parameter, and this estimate was used by Gutkin and Aifantis (1996, 1999a); Gutkin and Aifantis (1999b, 2000) in evaluating non-singular strain fields for dislocation and disclination arrangements and determining their interactions. As in the case of the phenomenological coefficient of the gradient plasticity theory based on Eq. (3.2), estimates for the coefficient $\bar{c}$ of gradient elasticity can also be obtained from fitting experimental data on size effects. This has been shown by the author (Aifantis, 1999a,b) (see also Tsagrakis, 2001, and references quoted therein) where size effects in torsion and bending of elastically deformed media with microstructure (polymeric foams, human bones) were modelled by gradient elasticity within a strength of materials approximation.

In concluding this discussion on the phenomenological gradient coefficients, it is pointed out that there are still some questions not only about their values but also on their signs depending on the local geometry and the local or global softening (instability) material or component behavior. Thermodynamics, local and global stability considerations, as well as uniqueness and well-posedness requirements for the solution of related

boundary value problems can provide insight to these questions. A generalized continuum thermodynamics framework allowing for an extra term in the energy equation to account for the internal work associated with the gradient terms was outlined by the author (Aifantis, 1984a). Since then, several papers have been written on the subject (e.g. Maugin and Muschik, 1994; Valanis, 1996; Polizzotto and Borino, 1998; Shizawa and Zbib, 1999; Menzel and Steinmann, 2000; Gurtin, 2000). The work of Gurtin (2000), in particular, provides the thermodynamic foundations of Eq. (3.2) and can be used as a guide to check the thermodynamic consistency of various physically motivated gradient plasticity models of this type.

3.2. The origin of gradient terms

Here we sketch some ideas pertaining to the origin of the gradient terms. In fact, it has been recently argued (Mughrabi et al., 2000) that in a number of important physical situations where scale effects are dominant, Ashby's concept of GND on which several (other type of) strain gradient theories are based upon (consult, for example the recent report of Fleck and Hutchinson (2001) and references quoted therein), is not relevant. Therefore, strain gradients may not be included in these cases on the basis of GND. Other physical mechanisms should then be involved. A brief discussion on such different sources for the gradient terms is outlined below.

3.2.1. Coupling with internal variables with diffusive transport

Instead of Eq. (3.2), one may start with a standard expression $\tau = \kappa(\gamma, \alpha)$ where α is an internal variable whose evolution equation contains both a rate and a flux term (Aifantis, 1987, 1992). For example, α may be identified with a dislocation population density evolving according to Eq. (3.1) with the strain γ entering as a parameter in the source term. Then, in a one-dimensional setting, we may assume $\dot{\alpha} = D\alpha_{xx} + \psi(\gamma) - \phi(\gamma)\alpha$ where (ψ, ϕ) are nonlinear functions of the plastic strain γ. By considering the Fourier transform of the linearized part of this equation and "adiabatically" eliminating the fast variable α (note that for

the spatial scales considered, α attains steady states much faster than γ), it turns out that α in the flow stress dependence $\tau = \kappa(\gamma, \alpha)$ is replaced by a second gradient term in γ. (Strictly speaking, the dependence of the internal variable α is replaced by a functional of γ which, under certain circumstances, results into a second gradient term. In fact, for a linear dependence of the form $\tau = \kappa(\gamma) - \lambda\alpha$, the resulting equation is of the form of Eq. (3.2) with $c = \lambda\Lambda D/M^2$; $\Lambda \equiv [\psi' - \phi'(\psi/\phi)]_{\gamma=\gamma_0}$, $M \equiv \phi(\gamma_0)$, with γ_0 denoting a uniform state, while the expression for the homogeneous part of the flow stress becomes $\kappa(\gamma) - \lambda\alpha_0(\gamma)$. where α_0 is the value of the internal variable when there are no gradients). By further assuming standard metal physics relations pertaining to the dislocation motion/multiplication mechanisms it is possible to obtain the following relation for the gradient coefficient c: $c = \beta h^2 D/\tau v$ where β is a numerical factor with an explicit dependence on the Burgers vector magnitude and the ratio of mobile to the total dislocation density, whereas the remaining symbols have their usual meaning (τ is the shear stress, h is the hardening modulus and D/v is an effective mean free path discussed earlier in this section). Typical values of the parameters involved for a slowly deforming Cu polycrystal give a value for the gradient coefficient $|c| \cong 10^{-3}$ N which is of the same order of magnitude as the one obtained from self-consistent models and size effect calibrations (Aifantis, 1995). Generally, a range between 1 and 10^{-3} N is obtained for c, depending on the deformation state and the average value of the effective mean free path swept by the moving dislocations, as well as the scale or the size of the elementary volume assumed for the problem at hand.

3.2.2. Statistical/randomness considerations

Another issue related to the phenomenological gradient coefficients and the scale considered, is concerned with statistical and randomness aspects associated with the microsructure. These considerations lead to gradient terms as sketched below. This is work in progress but some preliminary results have just been published or are pending publication (Avlonitis et al., 2001; Frantziskonis and Aifantis, 2002). By assuming that the strain $\hat{\gamma}(\Gamma)$ is a random field given by a function of a random microstrain variable Γ, a Taylor expansion around the mean $\langle\Gamma\rangle$ of the form $\hat{\gamma}(\Gamma) = \hat{\gamma}(\langle\Gamma\rangle) + \hat{\gamma}_\Gamma(\gamma - \langle\gamma\rangle) + 1/2\hat{\gamma}_{\Gamma\Gamma}(\Gamma - \langle\Gamma\rangle))^2$, and subsequent averaging yields the expression $\langle\hat{\gamma}(\Gamma)\rangle = \gamma = 1/2[(\partial^2 C(r)/\partial r^2)|_{r=0}]^{-1}\nabla_{rr}^2\langle\hat{\gamma}(\Gamma)\rangle$, where $\gamma = \hat{\gamma}(\langle\Gamma\rangle)$ and $C(r)$ denotes the spatial correlation (autocorrelation function) for the microstrains. For a Gaussian $C(r) = \exp[-(r/\ell)^2]$ autocorrelation function, it can be shown that $\langle\hat{\gamma}(\Gamma)\rangle = \gamma + (\ell^2/4)\nabla_{rr}^2\langle\hat{\gamma}(\Gamma)\rangle$ where ℓ denotes correlation length. Then, a constitutive equation of the form $\tau = \kappa(\gamma)$ can lead, through an appropriate Taylor expansion, to the gradient expression of Eq. (3.2) with γ now in Eq. (3.2) designating the average strain $\hat{\gamma}(\langle\Gamma\rangle)$ of the volume element. The sign of the coefficient c and its relation to the internal lengths involved, depend on the type of the correlation functions and the corresponding microstructures, as well as on the deformation state (hardening or softening). It also depends on the constitutive coarsening or the scale employed to express the constitutive equations. (For example, the above averaging procedure introduced to the constitutive equations $\tau = \kappa(\gamma)$ or $\tau = \kappa(\langle\hat{\gamma}(\Gamma)\rangle)$ would lead to the same gradient expressions but with different signs for the gradient coefficient, depending on the measure $\hat{\gamma}(\langle\Gamma\rangle)$ or $\langle\hat{\gamma}(\Gamma)\rangle$ used in the constitutive equation.)

4. Benchmark problems

In this section simple forms of gradient theory are employed to solve a number of critical problems with simple geometries for which, however, classical theory cannot predict the observed phenomena.

4.1. Interfaces

In relation to bi-material interfaces, gradient theory allows for a continuum distribution of strain across the interface. For two gradient linear elastic materials obeying Eq. (3.3), or equivalently Eq. (3.2) with $\kappa_i(\gamma) = \mu_i\gamma$, bonded by an elastic gradient interface and subjected to shear at infinity, it easily turns out that the strain distribution is given by the expression

$$\gamma = \frac{\tau^\infty}{\mu_i}\left[1 - \left(1 - \frac{\mu_i}{\mu_I}\right)e^{(-1)^i y \sqrt{\mu_i/c_i}}\right];$$
$$i = 1, 2, \tag{4.1}$$

where (μ_1, μ_2) and (c_1, c_2) are the shear moduli and gradient coefficients of the two bonded phases, while μ_I denotes an "elastic shear modulus" for the interface ($\tau_I = \mu_I \gamma_I$; τ_I and γ_I are the interfacial stress and strain) with $\tau_I = \tau^\infty$ (τ^∞ is the externally applied equilibrated stress), and y is the relevant spatial coordinate normal to the interface which is extended over the plane $y = 0$. For $\mu_I \equiv \mu_1 \mu_2 \times (\sqrt{\mu_1/c_1} + \sqrt{\mu_2/c_2})/(\mu_1\sqrt{\mu_2/c_2} + \mu_2\sqrt{\mu_1/c_1})$ we obtain the author's solution (Aifantis, 1995, 1996), while for $\mu_I \equiv \mu_1 \mu_2 (\sqrt{\mu_1 c_1} + \sqrt{\mu_2 c_2})/(\mu_1\sqrt{\mu_2 c_2} + \mu_2\sqrt{\mu_1 c_1})$ with $c_i = \mu_i \ell_i^2/2$ we obtain the solution of Fleck and Hutchinson (1993). The parameters ℓ_i ($i = 1, 2$) designate the corresponding internal lengths used in the Fleck/Hutchinson theory. The first solution was obtained for the boundary conditions $\partial\gamma_1/\partial y = \partial\gamma_2/\partial y$ at the interface, while the second solution was obtained for the boundary conditions $\ell_1^2\mu_1\partial\gamma_1/\partial y = \ell_2^2\mu_2\partial\gamma_2/\partial y$. ($\gamma_1$ and γ_2 denote the shear strains of each phase at the interface where we always have $\gamma_1 = \gamma_2 = \gamma_I$.) However, the problem of interest is to consider the nonlinear stress–strain behavior at the interface, as this problem relates to surface tension and crack nucleation. While the Fleck/Hutchinson theory is difficult to apply in this case, there is already a method available for considering this problem within the author's theory. In fact, for nonlinear behavior $\tau_I = \kappa(\gamma_I)$, it turns out that the strain distribution is determined by utilizing a Maxwell's equal area rule construction as discussed for fluid interfaces by Aifantis and Serrin (1983). The details of such construction will be shown elsewhere in relation to the problem of determining the thickness and strain distribution of coherent real interfaces. For the present illustrative purposes, it suffices to refer to the typical qualitative strain profiles given in Fig. 2, with τ_m designating the
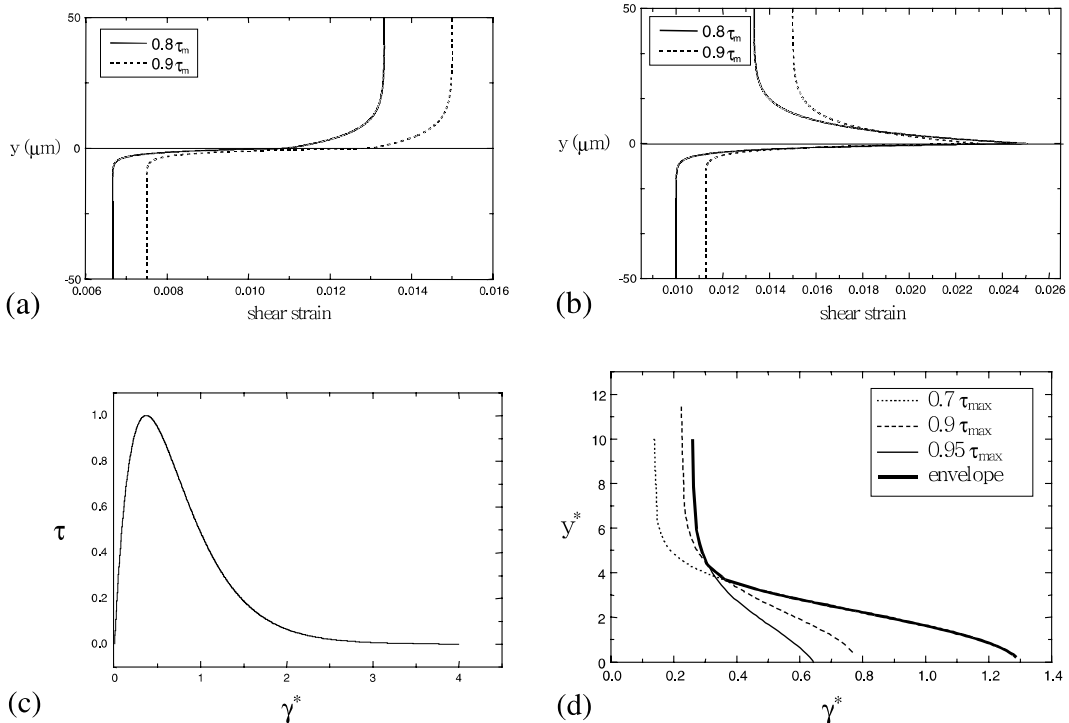

Fig. 2. Strain distribution across the interface for (a) $\gamma_I < \gamma_m$, (b) $\gamma_I > \gamma_m$, (c) scaled homogeneous universal stress–strain curve, (d) scaled universal strain distribution across the interface.

maximum value of stress in the corresponding cohesive type law for the interface and γ_m being the associated value of strain. It is noted that the strain profile is a transition when the strain at the interface is in the ascending branch (hardening) of the cohesive law, while it localizes when the strain at the interface is in the descending branch (softening). Results for real interfaces can be obtained by utilizing atomistic calculations by Rose et al. (1981, 1984) to motivate the expression for the "homogeneous" portion of the gradient-dependent constitutive equation. The resulting expression in scaled variables ($\tau^* = \tau/\tau_m e$ and $\gamma^* = (\delta^{eq}/\lambda)\gamma$) reads $\tau^* = \kappa(\gamma^*)\beta^2\gamma^* e^{-\beta\gamma^*}$, where β is a normalization constant, δ^{eq} is the equilibrium interface separation distance and λ is the range over which strong forces act. In Fig. 2 the "universal" scaled stress-scaled strain (τ^*–γ^*) curve and the corresponding universal scaled strain distribution across the interface of a metallic film bonded to a rigid substrate and sheared at infinity where it exhibits a rigid-like plastic behavior, are depicted in sketches (c) and (d) respectively.

4.2. Boundary layers

A related benchmark problem pointed out by Fleck (2000, 2001) is the shearing of a thin layer of material between two rigid plates. This problem was solved by employing several gradient plasticity models (including those proposed by Bassani, Parks, Gao and their co-workers), as well as by using the discrete dislocation dynamics (DDD)

formulation of Needleman/van der Giessen and co-workers. (Due to space limitations, we do not elaborate on details and do not list the appropriate references which can be found, however, in a recent report by Fleck and Hutchinson (2001).) It is noted, however, that the DDD approach requires substantial computational effort, but also the Fleck/Hutchinson model needs numerical implementation. On the contrary, the solution for the local shear strain γ based on Eq. (3.2) reads

$$\gamma(x_2) = \frac{\tau^\infty}{\mu} + \frac{\tau^\infty - \tau_Y}{h}\left[1 - \frac{\cosh(x_2/\ell)}{\cosh(H/2\ell)}\right], \qquad (4.2)$$

where $x_2 = y$ is the appropriate space coordinate ($-H/2 < x_2 < H/2$), H denotes the layer thickness, τ^∞ is the applied shear, μ is the shear modulus, h is the hardening modulus, τ_Y denotes the yield stress and the internal length ℓ is related to the gradient coefficient c of Eq. (3.2) by $c = h\ell^2$. Thus, Eq. (3.2) reads $\tau = \tau_y + h\gamma - h\ell^2\nabla_{yy}^2\gamma$, i.e. linear hardening is assumed. The global or macroscopic shear strain Γ can be calculated from Eq. (4.2) by direct integration and reads

$$\Gamma = \frac{1}{H}\int_{-H/2}^{H/2}\gamma(x_2)\,\mathrm{d}x_2$$
$$= \frac{\tau^\infty}{\mu} + \frac{\tau^\infty - \tau_Y}{h}\left[1 - \frac{2\ell}{H}\tanh\left(\frac{H}{2\ell}\right)\right] \qquad (4.3)$$

The corresponding local strain profiles and associated size effects are depicted in Fig. 3, where comparisons with the DDD simulations and the
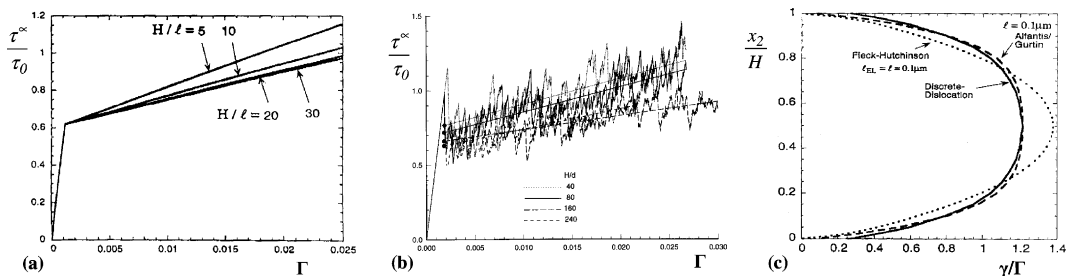

Fig. 3. (a) Effect of layer thickness H on the stress–strain curve response, as predicted by Aifantis–Gurtin theory. (b) Size effect, as predicted by discrete dislocation calculations indicating an elevation in flow strength with diminishing thickness H. (c) Shear strain (local) profile in 1 micron thick layer at a global shear strain $\Gamma = 0.0218$. It is shown that the author's theory is closer to the DDD simulations than the Fleck/Hutchinson theory. Some other recently proposed strain gradient models predict flat profiles and cannot capture boundary layer effects.

Fleck/Hutchinson predictions are provided (Fleck, 2000, 2001).

4.3. Size effects

The ability of the gradient theory to interpret size effects has already been shown above on the basis of the simple gradient plasticity model described by Eq. (3.2). Size effect data for twisted wires with dimensions at the μm regime, have been reported by Fleck et al. (1994). In order to fit their experimental data, the gradient-dependent flow stress given by Eq. (2.18) with $m = 2$ is employed. It is further assumed that $\kappa(\gamma) = \kappa_0\gamma^n, c_1 = (1/2)(dc_2/d\gamma), c_2 = c\gamma^{n-1}$; i.e. a power law expression is assumed for the homogeneous part of the flow stress and a similar relation is adopted for the gradient coefficients. The effect of first gradients of strain is accounted for, and the relation between c_1 and c_2 is required by the existence of an appropriate "plastic" potential. The corresponding expression for the twisting moment M reads

$$\frac{M}{\alpha^3} = 2\pi\left(\frac{\kappa_0}{n+3} + \frac{c}{2\alpha^2}\right)\gamma_s^n, \tag{4.4}$$

where $\gamma_s = \varphi\alpha$ denotes the surface strain with φ being the angle of twist per unit length and α being the wire radius. The experimental results are fitted very well by Eq. (4.4) for reasonable values of the material parameters involved. Fig. 4a depicts the comparison between theory and experiment with $\kappa_0 = 226$ MPa, $n = 0.2$ and $c = 9.1 \times 10^{-3}$ N for al cases but for $2\alpha = 20$ μm for which $c = 5.6 \times 10^{-3}$ N. If an internal length is defined by the relation $\ell_c = \sqrt{c/\kappa_0}$, then the corresponding values of ℓ_c for the above cases are 6.3 μm and 5 μm respectively. It is noted, in this connection, that the Fleck

and Hutchinson theory (Fleck and Hutchinson, 1993) gives an estimate for the internal length $\ell_c = 2.6$–5.1 μm without fitting the whole experimental regime.

The results depicted in Fig. 4a were obtained by using Eq. (2.18) within a strength of materials approximation where the geometry of the deformation field is assumed at the outset. With such type of approximation for the geometry of the deformation field, size effects and strain gradient hardening in micro indentation experiments can also be interpreted. This is illustrated in Fig. 4b and c: In Fig. 4b, the dependence of the hardness (H) on the indentation depth (h) is shown as predicted on the basis of Eq. (2.18), in comparison with the Fleck/Hutchinson (asymmetric stress) type theory and the experimental data of Nix and Gao (1998). In Fig. 4c, the dependence on the hardness (HV) at the center of a cylindrical specimen subjected to torsion is shown as a function of the angle of twist per unit length (φ); the comparison between experiment (Székely et al., 2001) and a simple analysis based on Eq. (2.18) is illustrated.

5. Plastic heterogeneity, length scales and wavelets

Fig. 5 confirms the heterogeneous character of plastic flow at the micrometer level. Fig. 5a and b are due to Engelke and Neuhauser (1995) and Brinck et al. (1998), while Fig. 5c for the shear strain was obtained (Konstantinidis, 2000) on the basis of the data of Fig. 5b for the slip height h. The relevant question here is how to quantify the highly heterogeneous profile of Fig. 5c. This was done (Konstantinidis, 2000) by employing a dis-
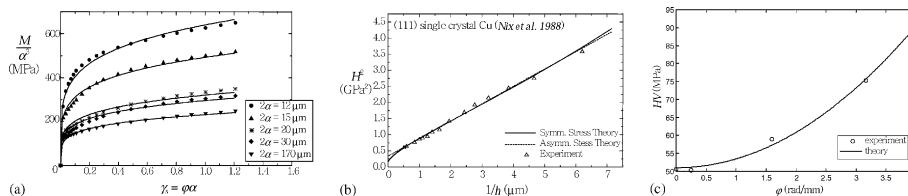

Fig. 4. Size effects (a) in torsion and (b) in indentation; strain gradient hardening is shown in (c). If size effects were absent or strain gradients effects were neglected, all curves in (a) would fall on a single curve and the slope in (b) and (c) would vanish as predicted by classical theory.
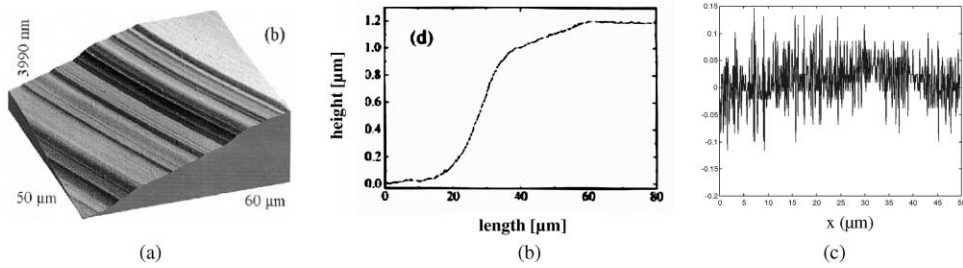
Fig. 5. Localized clustered slip bands in Fe$_3$Al appearing rapidly during deformation. (a) SFM micrograph of a typical section. (b) Step profile of the slip band shown in (a). The clustering of the steep part is about 25 perfect superdislocation Burgers vectors per 10^3 slip planes. (c) Strain distribution.
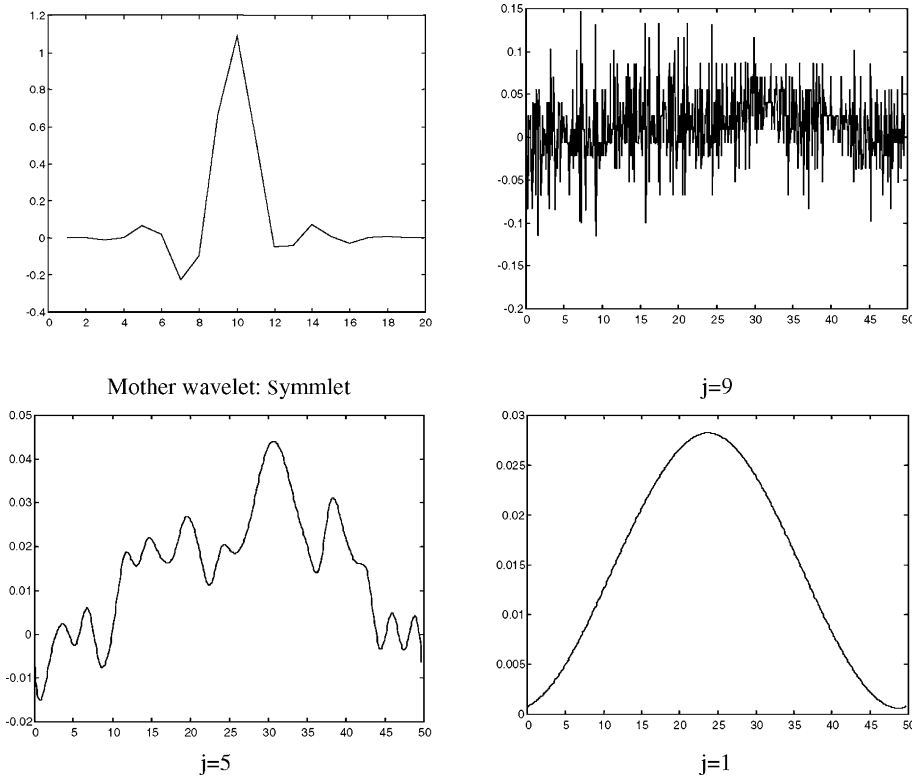

Fig. 6. Discrete wavelet transform for the strain distribution (scales $j = 1 \ldots 9$).

crete wavelet transform with a mother wavelet of the form $\Psi(x) \to \Psi_{j,k} = (1/\sqrt{2^j})\Psi[(x - 2^j k)/2^j]$ with $(2^{-j}, 2^j k)$ denoting the discrete dilatation and discrete translation respectively, while the index j denotes the scale. Fig. 6 shows the type of the mother wavelet used and the corresponding strain

profiles as the scale index j varies from 9 to 1. It is noted that for $j = 9$ (high resolution) the experimental strain profile of Fig. 5c is reproduced, while for $j = 1$ a shear band-like solution (small resolution) is obtained. These results were used to train a "neural network". On the basis of this, it was

possible to obtain the distribution of strain at smaller resolutions, not available experimentally, and infer on the heterogeneity of plastic flow at finer scales.

Another interesting result is obtained by attempting to relate the shear band profile (Fig. 6 for $j = 1$) with the shear band solution of the gradient theory (Aifantis, 1984b) through wavelet analysis. This is possible by employing a wavelet representation of the δ-function to represent the shear band solution. The appropriate form of this representation (Konstantinidis, 2000) is $\delta_s = (s_0/2s\sqrt{\pi})\exp[-x^2/4s^2]$ where s denotes the gage length and s_0 a macroscopic dimension of the specimen. It is then possible to replace the gradient term in Eq. (3.2) with a scale-dependent term. The final form of the resulting scale-dependent constitutive equation reads

$$\tau = \kappa(\gamma) - \frac{c\gamma}{2s^2}\left[1 + 2\ln\left(\frac{2s\sqrt{\pi}\gamma}{s_0}\right)\right]. \qquad (4.5)$$

More complex, but easy to obtain scale-dependent constitutive equations, are possible if the more general gradient expression given by Eq. (2.18) is used. These forms were utilized to model successfully the experimental data on size effects in torsion depicted in Fig. 4. They have also been used to interpret size effects in tension of homogeneously deforming smooth specimens with sub-millimeter and micrometer dimensions. These results will be reported in a future article where predictions of the gradient-dependent constitutive equation given by Eq. (3.2) and the scale-dependent given by Eq. (4.5) are compared with experimental data on size effects in torsion, bending and tension. Recent results based on Eq. (4.5) concerning the predictions of size effects in brittle materials and their comparison with the multi-fractal scaling laws proposed by Carpinteri and co-workers can be found in Konstantinidis et al. (2001).

Acknowledgements

References

Aifantis, E.C., 1982. Some thoughts on degrading materials. In: Atluri, S.N., Fitzerald, J.E., (Eds.), NSF Workshop on Mechanics of Damage and Fracture. Georgia Tech., Atlanta, pp. 1–12.

Aifantis, E.C., 1983. Dislocation kinetics and the formation of deformation bands. In: Sih, G.C., Provan, J.W. (Eds.), Defects, Fracture and Fatigue. Martinus-Nijhoff, The Hague, pp. 75–84.

Aifantis, E.C., Serrin, J.B., 1983. The mechanical theory of fluid interfaces and Maxwell's rule. J. Coll. Int. Sci. 96, 517–529 [see also Aifantis, E.C., Serrin, J.B., 1983. Equilibrium solutions in the mechanical theory of fluid microstructures. J. Coll. Int. Sci. 96, 530–547].

Aifantis, E.C., 1984a. Maxwell and van der Waals revisited. In: Tsakalakos, T. (Ed.), Phase Transformations in Solids. North-Holland, pp. 37–49.

Aifantis, E.C., 1984b. On the microstructural origin of certain inelastic models. J. Mater. Engng. Technol. (Trans. ASME) 106, 326–330.

Aifantis, E.C., 1984c. Remarks on media with microstructures. Int. J. Engng. Sci. 22, 961–968.

Aifantis, E.C., 1987. The physics of plastic deformation. Int. J. Plasticity 3, 211–247.

Aifantis, E.C., 1992. On the role of gradients on the localization of deformation and fracture. Int. J. Engng. Sci. 30, 1279–1299.

Aifantis, E.C., 1995. Pattern formation in plasticity. Int. J. Engng. Sci. 33, 2161–2178.

Aifantis, E.C., 1996. Non-linearity, periodicity and patterning in plasticity and fracture. Int. J. Non-Linear Mech. 31, 797–809.

Aifantis, E.C., 1999a. Gradient deformation models at nano, micro, and macro scales. J. Engng. Mater. Tech. 121, 189–202.

Aifantis, E.C., 1999b. Strain gradient interpretation of size effects. Int. J. Fract. 95, 299–314.

Aifantis, E.C., 2001. Gradient plasticity. In: Lemaitre, J. (Ed.), Handbook of Materials Behavior Models. Academic Press, New York, pp. 291–307 [see also Aifantis, E.C., 2000. Theoretical and experimental aspects of gradient theory, SEM IX International Con. Exp. Mech., Orlando, pp. 648–651, SEM].

Altan, B., Aifantis, E.C., 1992. On the structure of the mode III crack-tip in gradient elasticity. Scripta Met. Mater. 26, 319–324.

Altan, B.S., Aifantis, E.C., 1997. On some aspects in the special theory of gradient elasticity. J. Mech. Behavior Mater. 8, 231–282.

Avlonitis, M., Ioannidou, T., Frantziskonis, G., Aifantis, E.C., 2001. Statistical and stochastic aspects of gradient theory. J. Mech. Behavior Mater. 12, 77–84.

Bammann, D.J., Aifantis, E.C., 1982. On a proposal for a continuum with microstructure. Acta Mech. 45, 91–121.

Belytschko, T., Kulkarni, M., 1991. On the effect of imperfections and spatial gradient regularization in strain softening viscoplasticity. Mech. Res. Comm. 18, 335–343.

Brinck, A., Engelke, C., Neuhauser, H., Molenat, G., Rosner, H., Langmaack, E., Nembach, E., 1998. Dislocation processes in Fe_3Al investigated by transmission electron, scanning force and optical microscopy. Mater. Sci. Engng. A 258, 32–36 [see also Brinck, A., Engelke, C., Neuhauser, H., 1998. Quantitative AFM investigation of slip line structure in Fe_3Al single crystals after deformation at various temperatures, Mater. Sci. Engng. A 258, 37–41].

Cholevas, K., Liosatos, N., Romanov, A.E., Zaiser, M., Aifantis, E.C., 1998. Misfit dislocation patterning in thin films. Phys. Stat. Sol. B 209, 295–304.

Daubechies, I., 1992. Ten Lectures on Wavelets. SIAM, Philadelphia PA.

Engelke, C., Neuhauser, H., 1995. Static and dynamic strain ageing in $D0_3$—ordered Fe_3Al. Scripta Met. Mater. 33, 1109–1115 [see also Brinck, A., Engelke, C., Neuhauser, H., 1997. On the temperature dependence of slip inhomogeneity in Fe_3Al. Mater. Sci. Engng. A 234–236, 418–421].

Fish, J., Belsky, V., 1995. Multigrid method for a periodic heterogeneous medium. Part I: Convergence studies for one-dimensional case. Comp. Meth. Appl. Mech. Engng. 126, 1–16 [see also Fish, J., Belsky, V., 1995. Multigrid method for a periodic heterogeneous medium. Part 2: Multiscale modeling and quality control in mutidimensional case, Comp. Meth. Appl. Mech. Engng. 126, 17–38].

Fish, J., Chen, W., Nagai, G., 2002. Nonlocal dispersive model for wave propagation in heterogeneous media. Parts I, II. Int. J. Numer. Meth. Engng. 54, 331–363.

Fleck, N.A., Hutchinson, J.W., 1993. A phenomenological theory for strain gradient effects in plasticity. J. Mech. Phys. Solids 41, 1825–1857 [see also Fleck, N.A., Hutchinson, J.W., 1997. Strain gradient plasticity. In: Hutchinson, J.W., Wu, T.W. (Eds.), Advances in Applied Mechanics, 33, pp. 295–361].

Fleck, N.A., Müller, G.M., Ashby, M.F., Hutchinson, J.W., 1994. Strain gradient plasticity: Theory and experiment. Acta Metall. Mater. 42, 475–487.

Fleck, N.A., 2000. Nonlocal Plasticity. In: Solids Mechanics at the Turn of the Millenium (A Symposium Honoring J. Rice and J. Hutchinson) 15–16 June 2000, Brown University, Providence, RI.

Fleck, N.A., 2001. Private communication.

Fleck, N.A., Hutchinson, J.W., 2001. An assessment of a class of strain gradient plasticity theories, Harvard Report MECH 370, Harvard.

Frantziskonis, G., Loret, B., 1992. Scale dependent constitutive relations—Information from wavelet analysis and application to localization problems. Eur. J. Mech. A / Solids 14, 873–892.

Frantziskonis, G., Konstantinidis, A., Aifantis, E.C., 2001. Scale-dependent constitutive relations and the role of scale on nominal properties. Eur. J. Mech. A / Solids 20, 925–936.

Frantziskonis, G., Aifantis, E.C., 2002. On the stochastic interpretation of gradient-dependent constitutive equations. Eur. J. Mech. A / Solids 21, 589–596.

Gao, H., Huang, Y., Nix, W.D., Hutchinson, J.W., 1999. Mechanism-based strain gradient plasticity-I. J. Mech. Phys. Solids 47, 1239–1263 [see also Huang, Y., Gao, H., Nix, W.D., Hutchinson, J.W., 2000. Mechanism-based strain gradient plasticity-II, J. Mech. Phys. Solids 48, 99–128].

Gurtin, M.E., 2000. On the plasticity of single crystals: Free energy, microforces, plastic strain gradients. J. Mech. Phys. Solids 48, 989–1036.

Gutkin, M.Yu., Aifantis, E.C., 1996. Screw dislocation in gradient elasticity. Scripta Mater. 35, 1353–1358 [see also Gutkin, M.Yu., Aifantis, E.C., 1997. Edge dislocation in gradient elasticity. Scripta Mater. 36, 129–135].

Gutkin, M.Yu., Aifantis, E.C., 1999a. Dislocations and disclinations in gradient elasticity. Phys. Status Solidi 214B, 245–284.

Gutkin, M.Yu., Aifantis, E.C., 1999b. Dislocations in the theory of gradient elasticity. Scripta Mater. 40, 559–566.

Gutkin, M.Y., Mikaelyan, K.N., Aifantis, E.C., 2000. Screw dislocation near interface in gradient elasticity. Scripta Mater. 43, 477–484.

Hahner, P., 1996a. On the foundation of stochastic dislocation dynamics. J. Appl. Phys. A 62, 473–481.

Hahner, P., 1996b. A theory of dislocation cell formation based on stochastic dislocation dynamics. Acta Mater. 44, 2345–2352.

Konstantinidis, A., 2000. Applications of the Theory of Wavelets and Neural Networks to the Mechanical Behavior of Materials, PhD Thesis, Aristotle University of Thessaloniki.

Konstantinidis, A., Frantziskonis, G., Carpinteri, A., Aifantis, E.C., 2001. Size effects on tensile strength and fracture energy: Wavelets versus fractal approach. J. Mech. Behavior Mater. 12, 63–75.

Kubin, L.P., Devincre, B., 1999. From dislocation mechanisms to dislocation microstructures and strain hardening. In: Bilde-Sorensen, J.B. et al. (Eds.), Deformation-Induced Microstructures. Analysis and Relation to Properties. Riso National Laboratory, pp. 1–83 [see also Bulatov, V., Abraham, F.F., Kubin, L., Devincre, B., Yip, S., 1998. Connecting atomistic and mesoscopic simulations of crystal plasticity. Nature 391, 669–672].

Liosatos, N., Romanov, A.E., Zaiser, M., Aifantis, E.C., 1998. Non-local interactions and patterning of misfit dislocations in thin films. Scripta Mater. 38, 819–826.

Maugin, G.A., Muschik, W., 1994. Thermodynamics with internal variables. Part I: General concepts; Part II: Applications. J. Non-Equilib. Thermodyn. 19, 217–249, 250–289.

Menzel, A., Steinmann, P., 2000. On the continuum formulation of higher gradient plasticity for single and polycrystals. J. Mech. Phys. Solids 48, 1777–1796.

Mughrabi, H., Brown, M., Kubin, L., Kratochvil, J., Nabarro, F.R.N., Aifantis, E.C., 2000. Panel discussion on strain gradients. In: Plasticity of Materials—A Mature Paradigm or an Approaching Revolution? European Research Conference, 16–21 September, Acquafredda di Maratea, Italy.

Nix, W.D., Gao, H., 1998. Indentation size effects in crystalline materials: A law for strain gradient plasticity. J. Mech. Phys. Solids 46, 411–425 [see also references quoted therein].

Picu, R.C., 2002. The Peierls stress in non-local elasticity. J. Mech. Phys. Solids 50, 717–735 [see also Picu, R.C., 2002. On the functional form of non-local elasticity kernels, J. Mech. Phys. Solids 50, 1923–1939. Picu, R.C., Aifantis, E.C., in press. Atomistic models and gradient elasticity].

Polizzotto, C., Borino, G., 1998. A thermodynamics-based formulation of gradient-dependent plasticity. Eur. J. Mech. A/Solids 17, 741–761.

Romanov, A.E., Aifantis, E.C., 1993. On the kinetic and diffusional nature of linear defects. Scripta Met. Mater. 29, 707–712 [see also Romanov, A.E., Aifantis, E.C., 1994. Defect kinetics in crack instabilities. Scripta Mater. 30, 1293–1298; Gutkin, M.Yu., Romanov, A.E., Aifantis, E.C., 1995. Nonuniform misfit dilocation distributions in naoscale thin layers. Nanostructured Mater. 6, 771–774].

Romanov, A.E., Pompe, W., Mathis, S., Beltz, G.E., Speck, J.S., 1999. Threading dislocation reduction in strained layers. J. Appl. Phys. 85, 182–192 [see also Romanov, A.E., Pompe, W., Beltz, G.E., Speck, J.S., 1996. An approach to threading dislocation "reaction kinetics". Appl. Phys. Lett. 69, 3342–3344].

Romanov, A.E., Speck, J.S., 2000. Relaxation enhancing interlayers (REIs) in threading dislocation reduction. J. Electronic Mater. 29, 901–905.

Rose, J.H., Ferrante, J., Smith, J.R., 1981. Universal binding energy curves for metals and bimetallic interfaces. Phys. Rev. Lett. 47, 675–978 [see also Ferrante, J., Smith, J.R., 1985. Theory of the bimetallic interface. Phys. Rev. B 31, 3427–3434].

Rose, J.H., Smith, J.R., Guinea, F., Ferrante, J., 1984. Universal features of the equation of state of metals. Phys. Rev. B 29, 2963–2969.

Ru, C.Q., Aifantis, E.C., 1993. A simple approach to solve boundary value problems in gradient elasticity. Acta Mech. 101, 59–68 [see also Ru. C.Q., Aifantis, E.C., 1993, Unpublished Results].

Shizawa, K., Zbib, H.M., 1999. A thermodynamical theory of gradient elastoplasticity with dislocation density tensor. I: Fundamentals.. Int. J. Plast. 15, 899–938.

Sluys, L.J., de Borst, R., 1994. Dispersive properties of gradient and rate-dependent media. Mech. Mater. 183, 131–149 [see also Sluys, L.J., de Borst, R., Mühlhaus, H.B., 1996. Wave propagation, localization and dispersion in a gradient-dependent medium, Int. J. Solids Struct. 30, 1153–1171].

Székely, F., Groma, I., Lendvai, J., 2001. Statistical properties of dislocation structures investigated by X-ray diffraction. Mater. Sci. Engng. A 309–310, 352–355.

Tomita, Y., 1994. Simulations of plastic instabilities in solid mechanics. Appl. Mech. Rev. 47, 171–205.

Triantafyllidis, N., Aifantis, E.C., 1986. A gradient approach to localization of deformation. I. Hyperelastic materials. J. Elasticity 16, 225–238 [see also Triantafyllidis, N., Bardenhagen, S., 1993. On higher-order gradient continuum theories in 1-D nonlinear elasticity derivation from and comparison to the corresponding discrete models. J. Elasticity 33, 259–293].

Tsagrakis, I., 2001. The role of gradients in elasticity and plasticity—analytical and numerical studies. PhD Thesis, Aristotle University of Thessaloniki.

Unger, D.J., Aifantis, E.C., 1995. The asymptotic solution of gradient elasticity for mode III. Int. J. Fract. 71, R27–R32.

Unger, D.J., Aifantis, E.C., 2000. Strain gradient elasticity theory for antiplane shear cracks. Part I: Oscillatory displacements. Theor. Appl. Fract. Mech. 34, 243–252 [see also Unger, D.J., Aifantis, E.C., 2000. Strain gradient elasticity theory for antiplane shear cracks. Part II: Monotonic displacements, Theor. Appl. Fract. Mech. 34, 253–265].

Valanis, K.C., 1996. A gradient theory of internal variables. Acta Mech. 116, 1–14.

Walgraef, D., Aifantis, E.C., 1985. Dislocation patterning in fatigued metals as a result of dynamical instabilities. J. Appl. Phys. 58, 688–691.

Zaiser, M., Aifantis, E.C., 1999. Materials instabilities and deformation patterning in plasticity. Recent Res. Devel. Metall. Mater. Sci., Research Signpost 3, 79–103.

Zaiser, M., Aifantis, E.C., Avalanches in plastic deformation, J. Mech. Behavior Mater., in press. [see also Zaiser, M., Aifantis, E.C., 2001. Modeling the crushing of a cellular material. In: Aifantis, E.C., Kounadis, A.N. (Eds.), Proceedings of sixth National Congress of Mechanics, vol. 3, Giahoudi-Giapouli Publ., Thessaloniki. pp. 102–108].

Zbib, H.M., Aifantis, E.C., 1988a. On the structure and width of shear bands. Scripta Met. 22, 703–708 [see also Zbib, H.M., Aifantis, E.C., 1988. A gradient-dependent model for the Portevin-Le Chatelier effect, Scripta Met. 22, 1331–1336].

Zbib, H.M., Aifantis, E.C., 1988b. On the localization and post-localization behavior of plastic deformation—I, II, III. Res. Mech. 23, 261–305.

Zbib, H.M., Rhee, M., Hirth, J.P., 1998c. On plastic deformation and the dynamics of 3D dislocations. Int. J. Mech. Sci. 40, 113–127 [see also Zbib, H.M., Aifantis, E.C., 2003. Size effects and length scales in gradient plasticity and dislocation dynamics, Scripta Mater. 48, 155–160].